Point-by-point reply to all referee comments to manuscript AMT-2017-120

We thank all referees for their feedback and suggestions. Below we answer the reviews point-by-point followed by a marked up pdf that tracks changes in the manuscript (produced with latexdiff). The original referee's comments are written in black and the author's reply and changes to the manuscript are colored in blue/green respectively. References in green refer to the corrected manuscript and references in black (e.g. pagenumbers) refer to the original manuscript.

Author's reply to anonymous referee 1

p3/22 The exact wavelength should be given together with a measured and fitted spectrum. The spectral range and the spectral resolution are important elements to judge the analytical performance, also in the context of gas matrix effects. One may assume that the frequencies are as in (Geldern 2014), but the latter does not show a measured spectrum.

Author's response: Thanks for pointing this out. We added the information about the spectral region and the used absorption lines to the manuscript. We also added more details about the drying of the air sample and the spectral fit to the description of the instrument in the introduction.

Changes to the manuscript: We added this information to the introduction (page 3 line 12). We added chapter 2.3 about the spectrometer setup to the methods.

Water vapor may significantly impact the retrieved δ-values, either through spectral interference or through changes in absorption line characteristics (pressure broadening). If my understanding of the setup is correct, then humid samples were measured spectroscopically. Since this paper aims at validating a new spectrometer, it is vital to discuss and quantify the effect of changes in humidity.

Author's response/ Changes to the manuscript: The sample was dried with a Nafion drier before it was measured. This information was added to the manuscript, c.f. comment to p3/22.

(Along the same line) p3/23 describes the Delta Ray having "an internal calibration procedure that automatically includes two point calibrations for concentration c and both δ values as well as corrections for the concentration dependency of the measured d-values". This concept is interesting and a key feature of the Delta Ray. However, since this publication evaluates a commercial instrument, it should clearly describe the way concentration dependency is corrected (and how large it is) and to validate the procedure (accuracy, see above). This has not been achieved or is not presented.

Author's response/changes to the manuscript: We addressed this question by adding the chapter 'Evaluation of the calibration strategy', c.f. our comment to page p6/20, in especially Figures 4 and 5 in the revised manuscript. Additionally, we changed chapter 2.8.1 about the calibration procedure to provide more detailed information. (We changed the order or your comments here, because we refer to this chapter later.)

p4/12 physically different samples: There is no indication that the instrument was used in a batch mode configuration. In continuous flow mode (as the text suggests), mixing in the cell (and to some extend in the tubing) corresponds to a low-pass filter, which is fundamentally different to "physically different samples".

Author's response: We wanted to make sure, that we do not measure air samples that are majorly composed of the air masses in the previous measurement, thus we chose an averaging time that is larger than tau$_{5\%}$, yielding a situation in which less than 5% of the previous sample is mixed into the new sample (as $\tau_{5\%} = \tau_{10\%} \ln(0.05)/\ln(0.1) \approx 14$s, c.f. section 3.1.4). We agree that the formulation is

misleading and changed the sentence to:
Changes to the manuscript: We changed this to "consisting of four measurements each averaged for 20 s - thus the averaging time is longer than the instrument internal cell response time $\tau_{10\%}$ c.f. section 3.1.4"

p4/~~12~~20 "temporal stability" is not standard terminology and only used once in this paper. I suggest using "repeatability", following the international vocabulary of metrology (VIM) throughout the text.

Author's response/changes to the manuscript: We changed this terminology and use 'repeatability' throughout the text.

p6/20 Accuracy was tested by comparing with one (1) gas tank which was measured using an Aerodyne spectrometer. This part of the study is a key element and completely insufficient. The main challenge in laser spectroscopy is currently not (any more) precision but rather accuracy. There is no reason why anyone should trust another spectrometer (here Aerodyne) without a very detailed description of how the latter achieves traceability. Furthermore, accuracy will depend on at least two calibration scales, i.e. δ values and concentration. Therefore, the evaluation must (!) include measurements of traceable (likely IRMS) gases at different δ values and concentrations; otherwise it is an insufficient and somewhat random exercise. If this is not possible, then an alternative may be to use traceable standards and (!) field samples that are quantified in a traceable way. This is easily possible for $\delta^{13}C$ -CO_2, but more difficult for $\delta^{18}O$ -CO_2 because of the limited stability of the samples (see e.g. Tuzson 2007, DOI: 10.1007/s00340-008-3085-4).

Author's response:
Concerning the general concerns about our accuracy measurement with N=1: We changed the chapter about accuracy in the manuscript and included measurements with gas tanks at different concentrations (N=4) and δ values (N=4 for ^{13}C and N=5 for ^{18}O), see description below. Here, we also evaluate 'potential accuracy' as defined by (Tuzson 2007, DOI: 10.1007/s00340-008-3085-4).
Concerning the comparison to the Aerodyne instrument: We agree that it is problematic to use another laser spectrometer for comparison here. We additionally analyzed this tank with a Picarro (for CO_2 concentration) and IRMS (for δ values) at Max Planck Institute for Biogeochemistry in Jena. In the revised manuscript, we use only gas tanks that were measured at MPI in Jena, both: for calibration as well as measuring potential accuracy (c.f. Table 3).
Changes to the manuscript: We rewrote chapter 2.6 about Instrument characterization measurements to include additional measurements.
We removed the chapter "Accuracy" and replaced it by chapter 3.1.2 Evaluation of the calibration strategy.

p6/26 Measurement of the Allan plot was done in the lab because of limited gas supply in the field. This is not sufficient, because the goal of this study is characterization under field conditions. The argument of limited gas in the field is not convincing because at 80 ml/min, it would easily be possible to have many corresponding measurements of about 10 - 30 minutes, which, given an Allan Minimum at around 100 s, would be sufficient. A minimal approach would be to evaluate the 80 s target gas measurements. Alternatively, or in addition, one may use ambient conditions that are sufficiently stable (e.g. well mixed, afternoon, highest sampling port) to obtain at least a conservative estimate for the precision in the field. Finally, data from the PA tank measurement also give an indication of precision in the field.

Author's response: Thanks for these suggestions. We used the field measurements with the PA-tank to calculate Allan Deviations under field conditions at an averaging time of τ=1 s, yielding comparable values, c.f. table 4.

σ_A ^{13}C [ppm]		σ_A ^{18}O [ppm]		σ_A c [ppm]	
Lab	Field	Lab	Field	Lab	Field
0.29	0.34	0.40	0.44	0.09	0.09

Table 4: Comparison of Allan Deviations at 1 s averaging time based on field and lab measurements.

However, based on your questions about the calibration strategy (see comment to p6/20 above) and your comment about instrument characteristics under field conditions (see your comment to p1/4 below), we decided to add more lab measurements to this manuscript (e.g. measurements to evaluate the calibration scheme). Thus in the revised manuscript, we generally focus more on lab measurements to characterize the instrument.

Changes to the manuscript: We removed "under field conditions" in the abstract, and rewrote chapter '2.5 Instrument characterization measurements' see our answer to your comment to p6/20.

p7/30 Referencing was done at the concentration of the highest sampling port. Discuss the uncertainty resulting from the fact that some height had other concentrations, taking into account the "linearity calibration" (which does not test linearity but dependence of the retrieved δ values on c; a terminology that should be improved).

Author's response:

Concerning the terminology: We agree that the term "linearity calibration" is not very clear. We used this term because this is the name of the corresponding calibration procedure that can be found in the Delta Ray's manual as well as in the operational software. Thus, we think we should keep this terminology, to be consistent with the manual. To avoid misunderstandings, we replaced "linearity calibration" by "Correction of c-dependency (called 'linearity calibration' in the instrument's documentation and operational software)" at first occurrence and by "Correction of c-dependency ('linearity calibration')" for the following occurrences.

Concerning the uncertainties related to the referencing: We addressed this question by adding a chapter 'Evaluation of the calibration strategy', c.f. our comment to page p6/20, in particular Table 7 and Figure 4.

p8/1 This whole chapter is badly written and should be revised with respect to language. In addition, the arguments are not convincing. The concentration range of HS and LS is not any larger than the standards used in the first calibration (300 and 430 ppm). Choosing two out of five standards, that were meant to evaluate accuracy for calibration, leads to only three remaining standards that are perfectly bracketed. The mean and uncertainty at N=3 becomes then statistically very weak. Furthermore, the results for c also illustrate why using just one tank to assess the accuracy of the δ values is not sufficient and somewhat arbitrary (see p6/20 above).

Author's response: We originally introduced this post calibration because we found a large jump in the concentration measured with the target standard. No such jump occurred in δ values. The jump in the target concentration could be removed replacing the instrument internal calibration with the applied post calibration. We agree with you, that it is not convincing that this is related to the concentration range of the instrument internal calibration. We think that during this period there was a problem with the instrument internal concentration calibration. The reason is not very clear to us; it might be that we have a problem with target gas flow during this particular concentration calibration. After replacing this particular concentration calibration by the linear post calibration, the corresponding jump in the target standard disappeared.

Changes to the manuscript: We rewrote chapter 2.8.2 about the post calibration and applied it only for a time period in which we observed a jump in the target concentration.

p9/15: The authors state that they chose an averaging time of 20 s as compromise between number of measurements and precision. This is misleading or not clear enough. If there are no measurements of standards between 20 s intervals, then the precision does not mean much because the next mean value for 20s may have an excellent precision (given as SD) but may have drifted significantly, thus the two values with good precision cannot be compared at the level of their individual precision (it then becomes an issue of repeatability or accuracy, depending on the context).

Author's response: We removed this misleading description.

p9/20 "the mean deviation of N=300 field measurements of a tank with pressurized air" is a suitable way to quantify repeatability and should be compared (or moved) to the results found in the corresponding chapter 3.1.3. Unfortunately, the values are only given graphically in Fig. 3. However, looking at the difference of one (!) sample, one cannot determine accuracy of the spectrometer. Especially not for an analytical technique which is known to be strongly dependent on concentration and gas matrix. The test is thus not suited for its aim. This chapter and the next can be combined to determine repeatability (preferred terminology), and which - at least in the title - may be called long-term stability. However, it is critical to find a way to reliably determine accuracy.

Author's response/changes to the manuscript: See comment to p6/20 about the accuracy measurement.

p9/25 "sum of uncertainties". What the authors likely mean is the combined uncertainty or an uncertainty budget. However, this is not achieved by simple addition of the uncertainties, as suggested in the text. It is necessary to know what the authors consider for the individual uncertainty contributions (and why), what distribution they assume and – if the contributions are independent – how they calculate the combined uncertainty, and at what level of confidence they then express this combined uncertainty.

Author's response/changes to the manuscript: This section was removed, instead we discuss 'potential uncertainty' as defined by Tuzson 2008**.**

P10/7 The standard deviations of repeated measurements (0.2 ppm for CO_2 concentration and below 0.3‰ δ values) should be compared to literature values. For example, (Sturm 2013, amt-6-1659-2013) found repeated measurements of the same gas tank with a standard deviation which is a factor 4-7 better than the results shown here.

Author's response/changes to the manuscript: We added more lab measurements and discuss the repeatability in chapter 'Evaluation of the calibration strategy', including the comparison to literature data, please see our comment to your question p6/20. Here we added the following to the discussion – please note that these values slightly changed, because we removed two periods with known instrument problems (c.f additional footnote and new figure 7) and recalculated the post-calibration only for the time period in which we observed a problem with our target measurements. We changed the chapter 3.1.3 Repeatability during the field campaign. We added the following footnote2 on page 12.

Fig 5 What is the slope of the linear decay, and what process does it represent?

Author's response: We derived this linear relationship from a first order approximation for the theoretical (and unrealistic) assumption that no mixing occurs in the measurement cell. We added

the missing relevant information to the manuscript.
Changes to the manuscript: We added the missing information to the figure caption.

P1/9 “field conditions” This is ok, but only if sufficiently exhaustive to replace lab characterization.
Author’s response/changes to the manuscript: We changed this and included in general more lab measurements, c.f our comment to p6/20

P1/9 “accuracy of 0.1 ‰ for δ ^{13}C” how can this be smaller than repeated measurements?
Author’s response/changes to the manuscript: We changed the way how we quantified accuracy, c.f. our comment to p6/20. We changed the abstract to: “The potential accuracy (defined as the 1σ deviation from the respective linear regression that was used for calibration) was approximately 0.45ppm for c, 0.24‰ for ^{13}C and 0.3‰ for ^{18}O.”

P1/14 “became insignificant” Explanation needed (or explicit statement that no explanation found).
Author’s response: We are not sure which explanation is needed here a) the correlation itself or b) the change in the correlation coefficient from significant to insignificant? However, in the abstract, we just summarize the observed correlation and shifted the explanation into the discussion, because the discussion of both, a) and b) is a bit long.
Changes to the manuscript: “This correlation became insignificant (p>0.1) for the period after the first snow, indicating a decoupling of δ^{13}C of respiration from recent assimilates.”

p2/25 and 25: “isotopologues” isotopocules, or isotopologues and isotomers, or remove bracket.
Author’s response: We think it might be a bit confusing for the reader to use the term ‘isotopocule’ or add ‘isotopomer’ here, because the latter is irrelevant for CO_2- The Hitran database and many other authors use the the term isotopologue in this context (e.g. Kerstel and Giafriani 2008, Barbour 2011, Ellekoj 2013, Weh4013 ,Oikawa 2017 , Mohn 2007 ,Affek and Yakir 2014, Vardag 2014). However, we added the information about isotopomers in the footnote and tried to give a clearer definition of isotopoloues.

P2/32 Since this is already cited, check the references and cite them directly.
Author’s response/changes to the manuscript: We agree, but this part was removed anyway to shorten the introduction.

P3/9 The classification does not work for this instrument because it combines mid-IR with enhanced effective optical path length.
Author’s response: Thanks for pointing that out. We added another class of instruments in Table 2. However, this part of the manuscript was shortened a lot after we read the referees comments.

P3/20 “direct laser absorption spectrometer” direct absorption, not direct laser.
Author’s response/changes to the manuscript: We changed this to “laser based direct absorption spectrometer” throughout the text to be clearer.

P5/33 “purging pump to avoid condensation in the tubes” purging is ok, but why should it avoid condensation (except because of pressure drop).
Author’s response/changes to the manuscript: This was misleading, we changed this to: “We purged the main tube to reduce the time the air masses spend in the tubing. To avoid condensation, we heated the valve box (at which we expect a pressure drop) and the adjacent tubing.”
P6/5 “the tubes with this small flow rate and” Please explain why condensation is linked to flow rate.
Author’s response/changes to the manuscript: We removed this sentence.

P7/13 „linearity calibration“ It's not really about linearity but about concentration dependence of the retrieved d values.

Author's response/changes to the manuscript: We changed the terminology, see our answer to your comment to p7/30.

P9/14 Put in relation. Is this better/worse/comparable?
Author's response/changes to the manuscript: We changed this to: "we measured a comparable (slightly better) Allan Deviation below 0.03‰ (c.f. Table 5)."

Multiple comments to chapter 3.1.2
- there is no such thing as "expected uncertainty".
- "measured uncertainty" unsuited terminology
- in the context of the evaluation of a new analyzer you have to make sure that this is not a coincidence. (N=1).

Author's response/changes to the manuscript: We replaced this chapter by a chapter about the evaluation of the calibration strategy. Please see our answer to your comment about p6/20

P10/10 "instrument drift" It would be very interesting to know what the instrument drift is. However, the data shown here is the drift of the retrieved data after all (drift) corrections.
Author's response/changes to the manuscript: Thanks for pointing this out. As the remaining drift after all drift corrections does not seem a meaningful quantity, we removed this part of the data evaluation.

P10/13 "Turnover time" This implies that it is the "turnover" of a perfectly mixed reactor (cell). However, what you then determine are several elements; I suggest calling this "response time".
Author's response/changes to the manuscript: We changed "turnover time" to "response time".

P10/20 „to mixing of gas" please state whether the gas flow is turbulent under the given conditions.
Author's response/changes to the manuscript: The gas flow in all tubes is laminar with Reynolds numbers below 100 for all tubing (6mm and 1/16'). We added this information to chapter 2.5.

P13/3 "As soil respiration has been measured to account for around 80% of total respiration in an old beech forest in below 30 km distance to our field site (Knohl et al., 2008), we further focus on soil respiration and discuss the following hypothesis:" Please check if this is really the line of thought that you want to communicate.
Author's response: We changed this to "Because soil respiration has been measured to account for around 80% of ecosystem respiration in an old beech forest in below 30 km distance to our field site (Knohl et al., 2008), we assume that soil respiration dominates ecosystem respiration and thus we further focus on soil respiration and discuss the following hypothesis:"

P30/table 5 "not necessary; Figure with 1 s and minimum values is sufficient."
Author's response/changes to the manuscript: We would like to keep this table for the readers convenience.

P30/table 6 „not necessary; can be described in one sentence."
Author's response/changes to the manuscript: We removed this table and added the numbers directly into the text: "The analyzer's power consumption of approximately 220W was slightly smaller than the power consumption of the basic infrastructure of the setup that included the pump to purge the 9 inlet tubes and the heated valve box (330W)."

P30/table 7 "not necessary; text and Fig. 4 are sufficient."
Author's response/changes to the manuscript: We would like to keep this table for the readers convenience.

P33/21 “review language of this paragraph”
Author’s response/changes to the manuscript: We rewrote this paragraph.

Author’s reply to anonymous referee 2

1) The authors conclude in the abstract that “1) the new Delta Ray IRIS with its internal calibration procedure provides an opportunity to precisely and accurately measure c, $\delta^{13}C$ and $\delta^{18}O$ at field sites” I am concerned with this statement, because the internal calibration procedure in the IRIS is never actually described. How are the absorption spectra used to calculate isotope ratios, and how are these modified based on the calibration? This point appears critical for understanding whether the internal procedure is adequate and/or necessary, or for understanding what other post-hoc calibrations may be needed. This is a critical gap in the paper. Once cannot simply assume that the manufacturers of the instrument have worked out the details here. There are instruments that are sold that do not necessarily function as advertised, thus it is necessary to validate every step of the way. I would like to see plots and regressions of raw vs. known values for both $\delta^{13}C$ and $[CO_2]$ for a number of different standards spanning a broad range of δ values and mole fractions of CO_2 .

Author’s response: We added this missing information about the spectral fit, the calibration procedure and about the evaluation of the calibration procedure (including the suggested plots) to the manuscript.

Changes to the manuscript:
Changes to the manuscript: We added this information to the introduction (page 3 line 12). We added chapter 2.3 about the spectrometer setup to the methods. We changed chapter 2.8.1 about the calibration procedure to provide more detailed information and added chapter 2.6 that describes the additional measurements. We removed the chapter “Accuracy” and replaced it by chapter 3.1.2 Evaluation of the calibration strategy.

2) The authors mention that they used a post-hoc CO_2 concentration calibration, but it is unclear how often the additional standards used for this were measured (once? Halfhourly?) in relation to their check standard. Note that quadratic relationships may give a better fit as employed elsewhere for other absorption-based CO_2 instruments.

Author’s response: We originally introduced this post calibration because we found a large jump in the concentration measured with the target standard. No such jump occurred in δ values. The jump in the target concentration could be removed replacing the instrument internal calibration with the applied post calibration. We agree with you, that it is not convincing that this is related to the concentration range of the instrument internal calibration. We think that during this period there was a problem with the instrument internal concentration calibration. The reason is not very clear to us; it might be that we have a problem with target gas flow during this particular concentration calibration. After replacing this particular concentration calibration by the linear post calibration, the corresponding jump in the target standard disappeared.
Changes to the manuscript: Concerning the potential nonlinearity, Figure 5 in the revised manuscript evaluates the instrument’s linearity and quantifies the deviations from the linear regression, please see also the chapter “Evaluating the calibration strategy”. We rewrote chapter 2.8.2 about the post calibration and applied it only for a time period in which we observed a jump in the target concentration.

3) Given that this is a methods paper, it would have been very useful to see tests using a broader range of CO_2 mole fraction and isotope compositions in the range of standards, and to see more standards tested. Without this, we cannot validate the linearity of the instrument both in

concentration and isotope space. This is a critical deficit of the paper. Why was the need for a post-hoc δ^{13}C and δ^{18}O calibration not tested or described?

Author's response/changes to the manuscript: We addressed this questions by adding an additional chapter about test measurements to evaluate the calibration strategy. This chapter evaluates the concentration dependency of the δ values over a range of 200 to 1500 ppm and includes measurements of different gas tanks with concentrations ranging from (350 to 450 ppm) and isotopic compositions ranging from -37 to -9.7 ‰ for δ^{13}C and from -35 to -5 ‰ for δ^{18}O. Please see our response to question 1) above.

4) Note that many of the other laser-based isotope instruments achieve much higher precision with frequent (e.g. 20 minute) isotope calibrations in the field. This need appears especially critical here given the large (1 per mil) jumps in δ^{13}C values observed in the check standards shown in Figure 4. This suggests that there are some serious stability problems that need to be addressed with more frequent isotope calibration.

Author's response:

Concerning the large jumps in observed δ values: Thanks for pointing this out. We showed Figure 4 mainly to show the repeatability of the instrument, but we agree with you, that the large (1 ‰) jumps in δ values need more discussion. For these two large jumps, we found explanations: The first of these large jumps appeared in ^{13}C after calibration on 23th of September and disappeared after calibration on 29th of September. This jump only occurs in δ^{13}C of the target measurement. In particular, this jump was not visible in the δ^{13}C in the measurements of the different heights (see figure R1 for the highest inlet as an example). Thus, we conclude that there was a problem with ^{13}C calibration. This problem might be enhanced for δ values that deviate from the 'reference' δ value, in particular for the very depleted target measurement, that was even out of the calibration range.

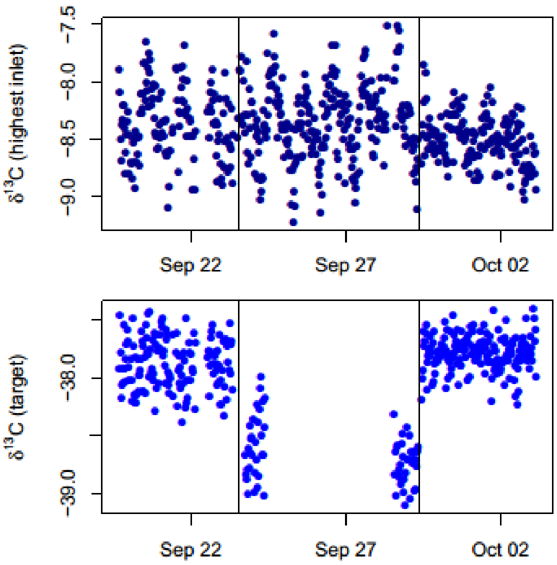

Figure R1 Time series of δ^{13}C values for the time period that shows a large jump in δ^{13}C for target measurements, but not for the height inlets, shown here as an example for the highest inlet.

The second large jump in the time series of the isotopic composition of the target gas from the 9th until the 16th of October includes the period during which we had a laser alignment problem and the laser needed to be readjusted. After calibration on 16th of October, the measured target gas value jumped back to its value before the 9th of October. We originally wanted to show all data points for completeness, but as we can relate them to a) a problem with one specific δ^{13}C calibration that occurs particularly for the very depleted target gas and b) a general laser alignment problem, we

think it is more appropriate to remove the corresponding data points from further analysis. In case of the laser alignment problem we also removed the corresponding time series of the height measurements.
Concerning precision, here we quantify precision by measuring the Allan deviation of the uncalibrated δ values, like many other authors (e.g. Sturm et al 2013, van Geldern et al 2014). For this comparison, Table 2 gives an overview about the precision of the δ value measurements of different laser-based and broadband light source-based instruments. In case you refer to what we called 'long-term-stability' in the original manuscript, but call 'repeatability' in the revised manuscript, this is discussed in the chapter 'Evaluation of the calibration strategy' (See our comment above).

Changes to the manuscript: We changed Figure 4/7 and the respective description to "Figure 7 Time series and frequency distributions of half-hourly measurements of the […] target gas [..]for the whole measurement period excluding periods that show problems with target gas flow, calibration and a laser alignment problem. Major reasons for data gaps are marked with different colors."
We added the chapter 3.1.3 "Repeatability during the field campaign**.**
We added the following footnote*: "In the case of ^{13}C, we excluded the target measurements between 23rd of September till 29th of September, because we obtained a problem with the ^{13}C calibration that lead to a large jump in the delta ^{13}C value of the (very depleted) target standard. This jump did not occur in the height measurements, probably because they were much closer to the reference delta value."

5) With respect to the second major conclusion of the abstract, "2) even short snow or frost events could have strong effects on the isotopic composition of CO_2 exchange at ecosystem scale" this finding is not new, but also not very well supported by the data (e.g. Figs 7 and 8. There are now several multi-year datasets of canopy CO_2 and $\delta^{13}C$ profiles in temperate ecosystems that have shown similar patterns.

Author's response:
Concerning conclusion 2) Here we summarize the results concerning ^{13}C as well as ^{18}O that are discussed in detail in the results section. This statement does not only refer to Figures 7 and 8. The parts of the manuscript that support this conclusion are in particular figure 9 (top panel) for ^{13}C and Table 8 for ^{18}O (in addition to figure 7). As we discuss in section 3.2.2, for ^{13}C we do not observe a change in the $\delta^{13}C$ values, but we find indications, that the processes controlling the ^{13}C of CO_2 exchange shifted. For brevity in the abstract, we tried to stay general, but specified this in the revised manuscript.
Concerning the mentioned multi-year records: We are well aware that there are now several multi-year records of ^{13}C and ^{18}O in CO_2 profiles (e.g. Bowling et al 2002b, Wehr et al 2016, Bowling et al 2003, Shim et al 2013). However, we are not so sure if the 'similar' pattern that you talk about show the same change in the time lagged (and negative) correlation between Reco^{13}C and 2-d averaged radiation (not VPD), particularly in the combination with frost events. It would be very interesting for us to see which species (^{13}C or ^{18}O) and which datasets you are referring to in particular and we are happy to include the respective citation
Changes to the manuscript: We specified the abstract "2) even short snow or frost events might have strong effects on the isotopic composition (in particular ^{18}O) of CO_2 exchange at ecosystem scale."
We added a more comprehensive list of citations, focussing on multi-year record to the introduction (page to page 2 line 12) "The temporal variability of the isotopic composition of respiration for example has been studied on timescales ranging from sub-diurnal (Barbour et al., 2011) to seasonal (Ekblad and Högberg, 2001; Bowling et al., 2002; Knohl et al., 2005). Further, the isotopic composition in CO_2 profiles has been studied on several sites over multiple years for ^{13}C (e.g. Bowling et al 2002b, Wehr 2016) as well as for ^{18}O (e.g. Bowling 2003, Shim et al 2013)."

We added a sentence referring to the observed peaks $R_{eco}{}^{18}O$ in the monsoon-dominated woodland observed by Shim et al to the discussion: "For comparison, similar strong peaks in $R_{eco}{}^{18}O$ have been observed in a semi-arid woodland after precipitation in New Mexico (Shim et al 2013), but this study refers to a monsoon dominated ecosystem with comparably large variability in the ^{18}O and does not focus on the difference of these pulses of snow and rain events."

6) With respect to the Keeling plot intercepts, no data is shown to actually validate the approach (e.g. plots of $\delta^{13}C$ and $1/CO_2$ space), nor summary statistics presented for these regressions. This is another serious deficit given the key methodological issues the authors point out in the Appendix, but do not quantify in the text. I don't think the authors present enough information here to rigorously test the hypotheses proposed in the Results/Discussion section.

Author's response: Below we show the histogram of R^2.

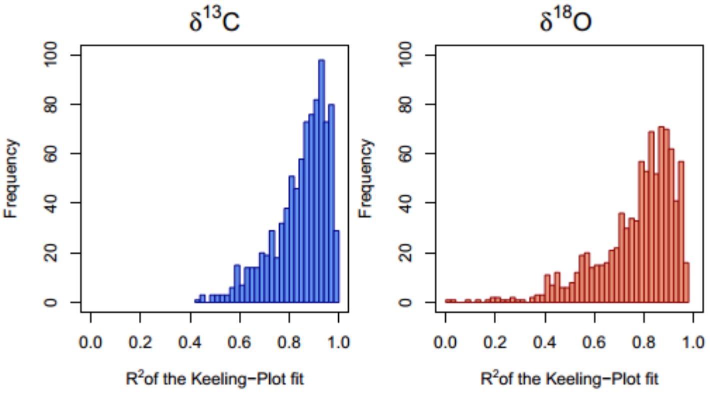

Figure R2 Histograms showing the R^2 values of accepted Keeling Plots based on data that was measured within 90 minutes during nighttime (between 20pm and 4 am).

Changes to the manuscript: We provide summary statistics about the regressions to the text: "The filtered nighttime Keeling-Plot intercepts based on 90 minutes of data acquisition had R^2 values with a median of 0.87 and 0.81 for ^{13}C and ^{18}O with mean values of 0.85 and 0.77 and standard deviations of 0.1 and 0.16 respectively."

We added the following Example Keeling-Plots to the supplementary material. We chose Keeling-Plots with R^2 values spanning the range of the respective mean+- 1 standard deviation.

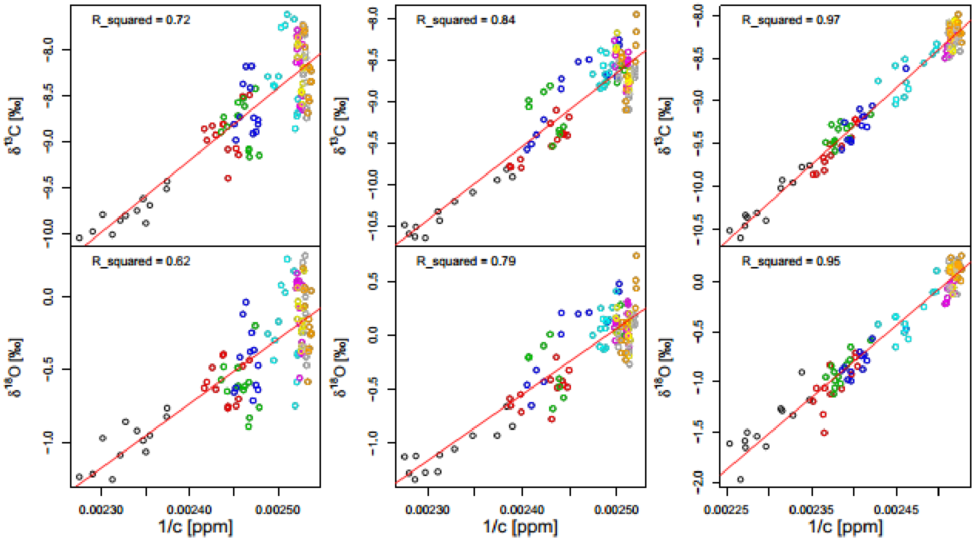

Figure S05 Example nighttime Keeling-Plots with typical R^2-values (spanning the range of the mean +- 1σ. Each Keeling-Plot is based on 90 min input data. Different colors represent different inlet heights.

The value of the CANVEG modeling exercise for the overall study was not terribly apparent to me, nor were the questions that it sought to address.

Author's response: We included the modelling to test the Hypothesis (a) (page 12 lines 1-14) as discussed in particular in lines 22ff. We modified this explanation to make the reason for the inclusion of the model clearer.

Changes to the manuscript: We added an additional sentence to the explanation in section 3.2.2 "Hypothesis (a):The variability of $R^{13}C$ eco can be partly explained by the isotopic composition of recent assimilates ^{13}C Ass, which is controlled by meteorological drivers during photosynthesis according to the Farquhar model. Thus, the variability of $R^{13}C_{eco}$ is linked to the variability of meteorological drivers of photosynthesis and photosynthetic discrimination with a time lag that is consistent with the time lag between respiration and assimilation. […We observed a correlation between radiation R_n and $R^{13}C_{eco}$,…] But the correlation itself cannot be directly explained by the Farquhar model of discrimination as radiation influences both, the CO_2 supply (by influencing stomatal conductance) and the CO_2 demand (by influencing assimilation) in the leaf (Farquhar and Sharkey, 1982). In particular, we did not find a significant time lagged positive correlation between $R^{13}C_{eco}$ and VPD, RH or the ratio VPD/PAR (Fig. 8), which could be directly associated with the Farquhar Model and has been found by the above mentioned studies. [this refers to (Ekblad and Högberg, 2001; Bowling et al., 2002; Knohl et al., 2005)] To test if it might be still reasonable to interpret the observed negative correlation of $R^{13}C_{eco}$ with Rn as a time lagged link between $R^{13}C_{eco}$ and isotopic composition of recently assimilated material $^{13}C_{Ass}$ on ecosystem scale, we performed a more complex calculation of $^{13}C_{Ass}$ by using the multilayer model CANVEG. The advantage of CANVEG is that it accounts for the non-linear interactions between air temperature, air humidity, radiation, stomatal conductance and photosynthesis."

To explain this thought earlier, we added/moved the following to the beginning of chapter 2.9: "To test if the measured variability of the $_{13}C$ composition of respiration can be partly explained by the variability of the $_{13}C$ composition of recent assimilates, we used the multilayer model CANVEG to simulate the isotopic composition of assimilated material during our measurement campaign. In particular, we analyzed the correlation of modeled $_{13}C_{Ass}$ to net radiation R_n, a driver of photosynthesis and photosynthetic discrimination, during our measurement period in autumn 2015.We further compared the resulting relationship between R_n and $_{13}C_{Ass}$ to the observed (time lagged) relationship between R_n and the $_{13}C$ composition of ecosystem respiration $R_{13eco}C$, derived from the measured

Keeling-Plots, c.f. section 3.2.2. This analysis was performed to test the hypotheses of a link between delta values in assimilated material and respiration."

7) More specific comments:

Introduction: there is much excessive detail here that repeats recent reviews, such as the Griffis 2013 paper. Please condense.

Author's response/changes to the manuscript: We shortened the introduction, in particular p2 line 22 ff.

P1 18: the main constraint is low temporal resolution

Author's response/changes to the manuscript: Thanks for pointing this out. We added this information to the manuscript.

P4 13: how are these "physically different" air samples if the pump is flowing continuously?

Author's response/changes to the manuscript: We removed this misleading description.

P8 5: "A possible reason for this resulting deviation is the range of the gas tanks we used for the instrument-internal concentration calibration, that was approximately 300 to 430 ppm" this logic doesn't make sense to me this is similar to your other standards
Author's response: We agree that this might not be the reason for the observed problems with concentration calibration, please see our answer to your comment 2).

P8 6: I am having trouble understanding how your "target standard" could be stable without posthoc calibration yet your five other standards were so variable.

Author's response: This was not the case. We found a need for post concentration calibration because the 'target' standard was not stable, please see our answer to your comment 2).

P8 9: "Secondly we set the IRIS analyzer's internal referencing procedure (described in Sect. 2.7) to 1800 s which corresponds to an Allan variance of 0.03 ‰ for both δ values and 0.01 ppm for CO_2 concentration." This is unclear to me are you measuring the standards every 1800 s? For how long?
Author's response: Yes, we measured the reference standard every 30 minutes. We measured it for 80s after the tubes were purged for 60s. We rewrote the chapter about the calibration procedure to be clearer (see our comment above).

Where are these new Allan variance values coming from?
Author's response: That was a typo. Thanks for finding it!

Figure 4: There are apparently large (1 per mil) jumps in measured "target gas" isotope values at several points. These are disconcerting. Are the data shown in this figure the raw values or the calibrated values? If they are the calibrated values, this suggests that the two-point calibration employed here is inadequate.

Author's response: The figure you are referring to (figure 4 in the original manuscript) shows calibrated values. Please see our answer to your comment number 4) above and the new chapter about the evaluation of the calibration strategy.

Author's reply to anonymous referee 3

1a) Page 2 lines 13ff: text passage about IRMS: Pls cite Schnyder et al. there (citation below)
1b) in the same text passage: I think "sample preparation effort and cost" might be a minus for IRMS techniques. But here the main disadvantages should be mentioned like (storage) problems with vials (see Gemery et al., 1996 and Knohl et al., 2004) and the advantage of quasi-continuous measurements relative to the "discontinuous" measurement by IRMS.
Author's response/changes to the manuscript: Thanks for these suggestions, we added this information to the respective paragraph: "IRMS has been widely used for isotope studies in environmental sciences, but shows limited applicability for *in situ* measurements (Griffis, 2013), but see also the field applicable continuous flow IRMS described by (Schnyder,2004). Disadvantages of flask-sampling based IRMS techniques include high sample preparation effort and costs (Griffis, 2013), low temporal resolution and discontinuous measurements. Additionally, there are potential problems during sample storage and transport, see (Knohl et al 2004) for minimizing such storage effects in case of ^{13}C. For ^{18}O storage effects can be related to oxygen exchange between water and CO_2 (Gemery 1996, Tuzson 2008)."

2) Page 2 lines 22ff. text passage about different spectrometer types: should be shortened as this manuscript is not a review on optical methods for measurement of isotope ratios
Author's response/changes to the manuscript: We shortened the introduction in especially page 2 lines 22ff.

3) Page 3 lines 25ff: "to characterize the Delta Ray IRIS and its performance under field conditions": I think measurement of the "internal cell turnover" and "Allan deviation" is not sufficient to fulfill this topic here. The reference gas box from the Delta Ray is said to offer possibilities to adjust CO_2 conc of the "reference" gas to the measured [CO_2] to cancel out a possible concentration effects on the measured d-values. The authors need to go more in detail here by showing data (!) from multiple CO_2-in air-standards with different [CO_2] and different $\delta\,^{13}$C-and d^{18}O values measured with IRMS (preferred) in comparison to measurement with Delta Ray or a comparison with different optical measurement devices (more problematic). I suppose you have measured the data, so show them here please.
Author's response: We show the measured concentration dependency as well as a comparison of multiple CO_2-in-air standards with IRMS measurements (δ values) and measurements with a Picarro (concentration) in figures 4,5, and 6.

We added chapter 2.6 '*Instrument characterization measurements'* to describe the additional measurements to the manuscript. We removed the chapter "Accuracy" and replaced it by chapter 3.1.2 Evaluation of the calibration strategy .

4) Please give more info (citation if available) on the kind of measurements performed at the MPIin Jena (isotopes and concentration).
Author's response/changes to the manuscript: We added this information to the manuscript: "All used CO_2 containing gas tanks were measured high precisely for their CO_2 concentration and isotopic composition in ^{13}C and ^{18}O at the Max Planck Institute for Biogeochemistry in Jena. There, the CO_2 concentrations were measured with a Picarro CRDS G1301 and the isotopic composition was measured with IRMS linked to VPDB (VPDP-CO_2) by using the multi point scale anchor JRA-S06 (Wendeberg et al 2013)."

5) The link to VPDP was done with the gas tank measured in Jena? Please extend the info on how this is done. Fig. 3 describes your quality control standard? Is there a way to compare measured values (+ stdev.) with a target value (+stdev.)?
Author's response:
Concerning the link to VPDB: We added a chapter that describes the calibration using the tanks that were measured in Jena.
Concerning Fig 3: We used the deviations between measured and target value with the respective

uncertainties to calculate accuracy in chapter 3.1.2. We changed this and used measurements with more than one tank to quantify ‘potential accuracy’ of the instrument. We added chapter 2.8.1 Instrument internal calibration to the manusctript.

6) Page 3 line 26 “b)” please add one or two sentences why $R_{eco}{}^{13}C$ and $R_{eco}{}^{18}O$is interesting.
Author’s response/changes to the manuscript: We added one more sentence to the first paragraph in the introduction. “The ^{13}C composition of ecosystem respiration $R_{eco}{}^{13}C$ on the one hand, has been used to assess the time lag between assimilation and respiration (e.g. Ekblad and Högberg, 2001; Bowling et al., 2002; Knohl et al., 2005) and to evaluate biosphere models on global scale (Ballantyne et al, 2011). The ^{18}O composition of ecosystem CO_2 exchange $R_{eco}{}^{18}O$ on the other hand is particularly interesting to study the coupled CO_2 and water cycle (see e.g. Yakir and Wang, 1996).”

7) Page 11 line 21 “lighter” here means only ^{13}C-depleted or also ^{18}O-depleted ? Please specify (also in whole manuscript)
Author’s response/changes to the manuscript: We specified this terminology throughout the manuscript.

8) Page 13 line 26: more “enriched” in what? Please check that also in whole manuscript, depleted in ^{13}C, enriched in ^{18}O (page 14 line 21...)
Author’s response/changes to the manuscript: We specified this terminology throughout the manuscript.

9) I‘m not totally happy to read a manuscript with 2 hypotheses where one hypothesis can be discarded but the 2nd one cannot be proven. The authors should find a way around this, at least the additional measurements for finally testing should be mentioned and discussed here.
Author’s response/changes to the manuscript: We added a paragraph that describes which measurements would be needed to support this hypothesis. These measurements are however very laborious, carry high uncertainty by themselves, and beyond the scope of this study. “To test this hypothesis, we would need to measure the amount and the isotopic composition of autotrophic respiration, total soil respiration and ecosystem respiration (e.g. by a trenching experiment) at our field site with an appropriate time resolution to capture the day-to-day variability during the field campaign. Lab measurements using incubations could also give an idea of the isotopic composition of autotrophic and total soil respiration, but would not fully reflect field site conditions. “

10) the unit “‰’ is not conform to the SI unit system, what about using “mUr”? It might be more an editorial decision
Author’s response: As ‰ is so commonly used and also the literature we are citing uses ‰, we think it might be most convenient for the reader is we also use ‰, even if it is not a SI unit. We are however happy to follow the editor’s suggestion.

We added the suggested references to the manuscript:

Gemery et al. (1996): Oxygen isotope exchange between carbon dioxide and water following atmospheric sampling using glass flasks. J Geophys Res 101, D9, 14514-14420.

Knohl et al. (2004): Kel-FTM discs improve storage time of canopy air samples in 10-mL vials for CO_2-$d^{13}C$ analysis. Rapid Comm Mass Spectrom. 18, 1663-1665.

Schnyder et al. (2004): Mobile, outdoor continuous-flow isotope-ratio mass spectrometer system for automated high-frequency ^{13}C- and ^{18}O-CO_2 analysis for Keeling plot applications. Rapid Comm Mass Spectrom. 18, 3068-3074.

A new instrument for stable isotope measurements of ^{13}C and ^{18}O in CO$_2$ - Instrument performance and ecological application of the Delta Ray IRIS analyzer

Jelka Braden-Behrens[1], Yuan Yan[1], and Alexander Knohl[1,2]

[1]University of Goettingen, Bioclimatology, Faculty of Forest Sciences and Forest Ecology, Germany
[2]University of Goettingen, Centre of Biodiversity and Sustainable Land Use (CBL), Germany

Correspondence to: Jelka Braden-Behrens (jbraden1@gwdg.de)

Abstract.

We used the recently developed commercially available Delta Ray Isotope Ratio Infrared Spectrometer (IRIS) to continuously measure the CO$_2$ concentration c and its isotopic composition δ^{13}C and δ^{18}O in a managed beech forest in Central Germany. Our objectives are (a) to characterize the Delta Ray IRIS and ~~its performance under field conditions~~ evaluate its internal calibration procedure and (b) to quantify the seasonal variability of c, δ^{13}C, δ^{18}O and the isotopic composition of nighttime net ecosystem CO$_2$ exchange (respiration) R^{13}_{eco}C and R^{18}_{eco}O ~~) derived from nighttime~~ derived from Keeling-Plot intercepts. The analyzer's minimal Allan deviation (as a measure of precision) was below 0.01 ppm for the CO$_2$ concentration and below 0.03 ‰ for both δ values. The potential accuracy (defined as the 1σ deviation from the respective linear regression that was used for calibration) was approximately 0.45 ppm for c, 0.24 ‰ for ^{13}C and 0.3 ‰ for ^{18}O. For repeated measurements of a target gas in the field, the long-term standard deviation from the mean ~~value was 0.2~~ was 0.3 ppm for c and below 0.3 ‰ for both δ values. ~~The accuracy based on our calibration setup was approximately 0.45 ppm for c, 0.1 for δ^{13}C and 0.6 for δ^{18}O.~~ We used measurements of nine different inlet heights~~in the beech forest~~, to evaluate the isotopic compositions of ~~respiration~~ nighttime net ecosystem CO$_2$ exchange R^{13}_{eco}C and R^{18}_{eco}O in a three months measurement campaign in a beech forest in autumn 2015. During this period, an early snow and frost event occurred, coinciding with a change in the observed characteristics of both R^{13}_{eco}C and R^{18}_{eco}O. Before the first snow, R^{13}_{eco}C correlated significantly (~~Pearson correlation coefficient $r_{\mathrm{pear}}\approx0.55$ and corresponding critical value $r_{\mathrm{crit}}\approx0.38$ for $\alpha=0.005$~~$p< 10^{-4}$) with time-lagged net radiation R_n, a driver of photosynthesis and photosynthetic discrimination against ^{13}C . This correlation became insignificant $(p> 0.1)$ for the period after the first snow, indicating a decoupling of δ^{13}C of respiration from recent assimilates. For ^{18}O, we measured a decrease of 30 ‰ within 10 days in R^{18}_{eco}O after the snow event, potentially reflecting the influence of ^{18}O depleted snow on soil moisture. This decrease was ten times larger than the corresponding decrease in δ^{18}O in ambient CO$_2$ (below 3 ‰) and took three times longer to recover (three weeks vs. one week). In summary, we conclude that 1) the new Delta Ray IRIS with its internal calibration procedure provides an opportunity to precisely and accurately measure c, δ^{13}C and δ^{18}O at field sites and 2) even short snow or frost events ~~could~~ might have strong effects on the isotopic composition (in particular ^{18}O) of CO$_2$ exchange at ecosystem scale.

1 Introduction

The stable isotopic compositions of CO$_2$ and water vapor have been intensely used to study ecosystem gas exchange (Yakir and Sternberg, 2000). In particular, measurements of the δ^{13}C and δ^{18}O isotopic composition of CO$_2$ have provided important insights into the carbon cycle over a large variety of spatial and temporal scales (Flanagan and Ehleringer, 1998; Affek and Yakir, 2014). There are many examples for the utility of the stable isotopic composition of CO$_2$ to study biosphere-atmosphere exchange processes on ecosystem scale, such as the partitioning of net ecosystem CO$_2$ exchange into respiration and photosynthesis. Different partitioning methods include the combination of gradient approaches with stable isotope measurements (Yakir and Wang, 1996), direct ~~isotopologue~~ isotope gradient approaches (Zhang et al., 2006), the combination of eddy covariance measurements with isotope flask measurements (Bowling et al., 2001; Ogée et al., 2003; Knohl and Buchmann, 2005), and direct isotope eddy covariance measurements ~~for isotopologues . Another example for the use of stable isotopes in~~ (Wehr et al., 2016; Oikawa et al., 2017). Other field applications of stable CO$_2$ ~~to investigate ecosystem gas exchange, is the analysis of the~~ isotopes measurements investigate the temporal variability of the isotopic composition of a particular flux component. The temporal variability of the isotopic composition of respiration for example has been studied on timescales ranging from sub-diurnal (Barbour et al., 2011) to seasonal (Ekblad and Högberg, 2001; Bowling et al., 2002; Knohl et al., 2005). ~~The mentioned studies on seasonal scale also used the temporal variability of the isotopic composition of respiration~~ Further, the isotopic composition in CO$_2$ profiles has been studied on several sites over multiple years for ^{13}C (e.g. Bowling et al., 2002; Wehr et al., 2016) as well as for ^{18}O (e.g. Bowling et al., 2003b; Shim et al., 2013). The ^{13}C composition of ecosystem respiration $R_{eco}^{13}C$ on the one hand, has been used to assess the time lag between assimilation and respiration (Ekblad and Högberg, 2001; Bowling et al., 2002; Knohl et al., 2005) and to evaluate biosphere models on global scale (Ballantyne et al., 2011). The ^{18}O composition of ecosystem CO$_2$ exchange $R_{eco}^{18}O$ on the other hand is particularly interesting to study the coupled CO$_2$ and water cycle (see e.g. Yakir and Wang, 1996).

A long established and broadly used technique to measure stable isotopic compositions is Isotope Ratio Mass Spectrometry (IRMS) ~~, with~~ (Griffis, 2013), a technique that is based on the fact that moving ions with different mass-to-charge ratio can be separated by (orthogonal) magnetic fields (Thomson, 1908). For measurements of the isotopic composition of CO$_2$, IRMS has typical precisions of approximately 0.02 to 0.1 ‰ for ^{13}C and 0.05 to 0.2 ‰ for ^{18}O~~in CO$_2$. In general, the concept of mass spectrometers, developed by , is based on the fact that moving ions with different mass-to-charge ratio can be separated by (orthogonal) magnetic fields.~~ . IRMS has been widely used for isotope studies in environmental sciences, ~~but~~ though it shows limited applicability for *in situ* ~~meteorological measurements - reasons for this~~ measurements (Griffis, 2013) , but see also the field applicable continuous flow IRMS described by Schnyder et al. (2004). Disadvantages of flask-sampling based IRMS techniques include high sample preparation effort and costs (Griffis, 2013)~~. ~~, ~~Progress in optical based techniques for isotopic measurements~~ low temporal resolution and discontinuous measurements. Additionally, there are potential problems during sample storage and transport, see Knohl et al. (2004) for minimizing such storage effects in case of ^{13}C. For ^{18}O storage effects can be related to oxygen exchange between water and CO$_2$ (Gemery et al., 1996; Tuzson et al., 2008). Optical based techniques can compete with or complement IRMS measurements and progress in optical based techniques over the last decade enhanced the potential of measurements of isotopic compositions (Werner et al., 2012). These developments have a particular impact on micrometeorological studies, as they increased the accessibility of field-deployable optical instruments and thus enabled a number of micrometeorological applications of stable isotope techniques, as reviewed by Griffis (2013).

Optical instruments to study the isotopic composition of trace gases use the absorption of infrared photons by exciting a ~~molecules~~ molecule's rotational and vibrational energy states. These rotational and vibrational transitions are characteristically different for ~~molecules, composed of different stable isotopes (isotopologues) .~~isotopologues, defined e.g. by Coplen (2011) as 'molecular species that differ only in isotopic composition', (see e.g. Esler et al., 2000; Kerstel and Gianfrani, 2008)[1]. The ~~characteristic absorption lines for the different isotopologues of a molecule~~ isotopologue-specific absorption lines are related to the ~~isotopologues concentrations~~ concentration of the respective isotopologue via Beer's law and thus the isotopic composition of a certain molecule (Werle, 2004). ~~The available~~ Available optical instruments that are capable of measuring isotopic compositions at trace gas concentrations show different implementations of this principle ~~: One major classification of optically based instruments can be done with respect to the light source that is used, between 1. broadband light source based instruments and 2. laser based instruments . Fourier Transform Infrared (FTIR) Spectrometers, as e.g. the Spectronus analyzer~~ ~~*Ecotech Pty Ltd., Knoxield, Australia*~~ ~~, belong to the first of these categories. In these kind of instruments, the complete infrared spectrum of a black body light source is used . The emitted infrared light is modulated by a Michelson interferometer andthe resulting interferogram is recorded and converted into the absorption spectrum mathematically by applying a Fourier transformation (, citing and). In laser based absorption spectrometers on the other hand, a laser beam with tunable wavelength is sent through a (~~(by using different light sources (broadband light sources, mid or near infrared lasers) (see e.g. Griffis, 2013; Kerstel and Gianfrani, 2008) and/or different absorption cells (multi-path or resonant) ~~absorption cell, usually operating at low pressure, and the light intensity of the emerging laser beam is measured by a suitable detector~~ (Werle, 2004). ~~Laser based instruments have been described in detail by , who provide a further classification for laser-based measurements at trace gas concentrations. In slightly different words, these categories can be named (a) direct laser absorption spectrometers in mid infrared where strong absorption features are available and (b) laser absorption spectrometers in near infrared that compensate the weaker absorption in the near infrared by a strongly enhanced effective optical path length.~~

~~Different laser spectrometers of the above mentioned category of instruments 2.(a) use different lasers to achieve a laser beam in the desired mid infrared region . Examples for such different laser types in laser absorption spectrometers are the quantum cascade lasers in QCLAS-instruments,~~ ~~*Aerodyne Research. Inc, Boston, USA*~~ ~~and CCIA-48~~ ~~*Los Gatos Research. Inc, San Jose, USA*~~ ~~, or the lead-salt tunable diode lasers, in the TGA100A/200 instruments,~~ ~~*Campbell Scientific Inc., Logan, USA*~~ ~~. For instruments of class 2.(b) there are two major technical implementations that both increase the optical path length by using high finesse optical cavities yielding a better signal-to-noise ratio . Both of these implementations are related to the decay of light intensity after the laser is switched of : Cavity Ringdown Spectroscopy (CRDS), e.g. the G1101-i and G1101-i+~~ ~~*Picarro Inc.,Santa Clara, USA*~~ ~~see e.g. , and Off-Axis Integrated Cavity Output Spectroscopy (OA-ICOS), e.g. the CCIA DLT-100~~ ~~*Los Gatos Research Inc., San Jose, USA*~~ ~~see e.g. .~~ Minimal Allan deviations σ_A and the corresponding averaging times $\tau_{\min}$ for

---

[1] In general this is also true for isotopemers, defined e.g. by Coplen (2011) as 'molecular species having the same number of each isotopic atom […] but differing in their positions.', (e.g. Mohn et al., 2008).

different optical ~~based instruments of all three different categories~~ instruments are shown in Table 2, but see also Table 2 in the review of Griffis (2013) for more detailed information, including instrument stability and an overview of applications, for most of these instruments.

Here we present a new laser based ~~instrument~~direct absorption spectrometer in the mid infrared, the Isotope Ratio Infrared Spectrometer (IRIS) Delta Ray ~~,~~*Thermo Scientific Inc., Waltham, USA*~~, that belongs to category 2.(a): A direct laser absorption spectrometers in mid infrared~~. This spectrometer uses ~~a nonlinear crystal in combination with~~ two tunable near infrared diode lasers in combination with a nonlinear crystal to produce a laser beam in the mid infrared ~~, at approximately 4.3~~ (Thermo Fisher Scientific, 2014). The instrument scans a spectral region from 4.3293 μm to 4.3275 μm, containing four CO_2 absorption lines: at 4.3277 μm ~~. The~~ and 4.3280 μm (both for $^{16}O^{12}C^{16}O$), 4.3283 μm (for $^{16}O^{13}C^{16}O$), and 4.3286 μm (for $^{16}O^{12}C^{18}O$) (Geldern et al., 2014). A measured and a fitted spectrum is shown in Fig. 1. The fitting procedure is based on a Voigt-Profile fit, that relates the isotopologue-specific absorption lines to their respective concentrations (information from the manufacturer, Thermo Fisher Scientific). The instrument has a flow rate of 0.08 slpm, a cell pressure of approximately 100 mbar, an optical path length of approximately 5 m and an internal calibration procedure that automatically includes two point calibrations for concentration c and both δ values as well as corrections for the concentration dependency of the measured δ-values (Thermo Fisher Scientific, 2014). The objectives of our study are (a) to characterize the Delta Ray IRIS and its performance under field conditions as well as (b) to quantify the seasonal variability of δ^{13}C, δ^{18}O and the isotopic composition of CO_2 exchange for both δ^{13}C and δ^{18}O derived from Keeling-Plot intercepts. ~~We measured the internal cell turnover to capture the maximum sampling frequency of physically different samples. Additionally, we measured the Allan deviation to assess the instruments precision and performed accuracy measurements using a gas tank with known isotopic composition. We assessed long-term stability of the instrument by performing repeated tank measurements. For the ecological application, we installed the instrument in a beech forest in Central Germany, characterized the seasonal variability of the isotopic composition of~~ ~~CO_2~~ ~~exchange (~~~~R^{13}_{eco}~~~~C and~~ ~~R^{18}_{eco}~~~~O), and analyzed the correlation between the seasonal variability of~~ ~~R^{13}_{eco}~~~~C and different meteorological variables.~~

2 Material and methods

2.1 Field site

This study was conducted at a meteorological tower in a managed beech forest (*Fagus sylvatica L.*) in Thuringia (Central Germany) at 51°19’41,58” N; 10°22’04,08” E at 450 meters above sea level. The forest in the dominant wind direction of the tower has ~~a~~ an average canopy height of approximately ~~35~~34 m with approximately 120 year old trees, a top-weighted canopy and a ~~very~~ homogeneous stand structure~~containing~~ , surrounded by trees of three age classes (approximately 30–40, 80 and 160 years)~~.~~, (Anthoni et al., 2004). The field site is described in detail by Anthoni et al. (2004), and soil characteristics of this site were analyzed by Mund (2004).

2.2 Campaign design

We measured the CO_2 concentration c and its isotopic composition δ^{13}C and δ^{18}O in ambient air from ~~21.~~ 21^{st} August 2015 to ~~16.~~ 16^{th} November 2015. We measured these quantities with the field deployable Isotope Ratio Infrared Spectrometer (IRIS) Delta Ray (*Thermo Scientific, Waltham, USA*) at nine inlet heights ranging from 0.1 to 45 m in an automatic measurement setup. ~~Each~~ After the tubing was purged for 60 s, each inlet was measured for 80 s, (consisting of four ~~physically different air samples, averaged over~~ measurements each averaged for 20 ~~s separately) after the tubing was purged for 60 s.~~s - thus the averaging time is longer than the instrument internal cell response time $\tau_{10\%}$ c.f. section 3.1.4). A full measurement cycle took 30 minutes and consisted of measurements of all nine inlet heights and a target standard ~~(CO~~with known CO_2~~in synthetic air with known~~ concentration and isotopic composition ~~, details for the gas tank are given in Sect. 2.5~~(CO_2 in synthetic air, tank 'SA-CO_2-5 in Table 3), supplemented by an internal calibration measurement~~.~~, called 'referencing' (c.f. Sect. 2.8). In less detail, the experimental setup is also described in (Braden-Behrens et al., 2017).

We used the nighttime measurements of c, δ^{13}C and δ^{18}O of the different inlet heights in a Keeling-Plot approach (Keeling, 1958) to calculate the nighttime Keeling-Plot intercept that can be used to estimate the isotopic composition of ~~ecosystem respiration~~ nighttime net ecosystem CO_2 exchange (respiration) δR_{eco} for both measured δ values: ^{13}C and ^{18}O. Additionally, we used the half hourly measurements of the target standard to track the ~~temporal stability~~ repeatability of the Delta Ray analyzer and performed additional (manual) measurements ~~to analyze the analyzer's characteristics.~~ characterize the analyzer.

2.3 Spectrometer setup

We set up the spectrometer to use the absorption lines at 4.3277 μm (for $^{16}O^{12}C^{16}O$), 4.3283 μm (for $^{16}O^{13}C^{16}O$), and 4.3286 μm (for $^{18}O^{12}C^{16}O$). Thus, only three of the four absorption lines in the instrument's measured spectra (Fig. 1), were used for the spectral fit. In particular, for $^{16}O^{12}C^{16}O$, we did not use the strong absorption line at 4.3280 μm. The corresponding mode of operation is called 'high concentration mode' in the instrument's operational software QTEGRA. Additionally, the sample was dried before it entered the measurement cell with the (instrument's internal) Nafion drier.

2.4 Application of the Keeling-Plot approach

The Keeling-Plot approach (Keeling, 1958) is based on a simple two-component mixing model that describes how air from a source with effectively constant isotopic composition δ_s mixes with a background (with constant c_{bg} and δ_{bg}). For this simple two-component mixing model, one can derive a linear relationship between the measured isotopic composition δ_{meas} and the reciprocal concentration $1/c_{\mathrm{meas}}$ by applying conservation of mass for the total concentration as well as for each isotopologue separately, for derivation ~~see e. g. .~~ (see e.g. Pataki et al., 2003).

$$\delta_{\mathrm{meas}} = \underbrace{(\delta_{bg} - \delta_s)\, c_{bg}}_{m_{\mathrm{KP}}} \frac{1}{c_{\mathrm{meas}}} + \underbrace{\delta_s}_{\delta_{\mathrm{KP}}} \tag{1}$$

This linear relationship with slope m_{KP} and intercept δ_{KP} can be derived for each isotopic species independently, so in our case for both δ^{13}C or δ^{18}O. The applicability of the Keeling-Plot approach to a certain experimental setup essentially depends on the question if c_{bg}, δ_{bg} and δ_s are ~~effectively~~ constant over the spatial and temporal distribution of all measurements that are taken into account for the linear regression. In this study we apply a Keeling-Plot approach to a forest ecosystem, aiming at measuring the isotopic composition of ecosystem integrated CO_2 exchange. The source of CO_2 is thus composed of different individual source components i (e.g. stem, leaf and soil respiration), each accounting for the individual components with their isotopic compositions $\delta_{s,i}$. The corresponding isotopic composition of the integrated source δ_s can be expressed by defining α_i, as the relative contributions of the individual source components to the integrated source.

$$\delta_s = \sum_i \delta_{s,i}\,\alpha_i \qquad \text{with:} \qquad \sum_i \alpha_i = 1 \tag{2}$$

If the relative distributions among the different source components α_i produce significant changes in δ_s over the spatial and temporal distribution of measurements, the basic two component assumption of stable δ_s is violated. During daytime the application of a Keeling-Plot approach on ecosystem scale in a forest is in general problematic, as photosynthesis and respiration are two separately controlled and spatially separated processes - so we generally can not assume spatiotemporally constant α_i. But for nighttime, when there is only respiration, the nighttime Keeling-Plot intercept δ_{KP} can be interpreted as the isotopic composition of ~~respiration~~ nighttime net ecosystem CO_2 exchange (respiration) $\delta^{13}\mathrm{C}\,R_{\mathrm{eco}}$ or $\delta^{18}\mathrm{O}\,R_{\mathrm{eco}}$. Measures to assure and test the applicability of this two component approach and to improve the quality of the calculated Keeling-Plot intercepts are discussed and evaluated in appendix A. In brief, they include the minimization of the sampling time for each Keeling-Plot, an inclusion of all inlet heights into each Keeling-Plot analysis to increase the CO_2 concentration range, data filtering and weighted averaging of Keeling-Plots on smaller timescales.

2.5 Material and technical specifications

Technical specifications of the setup including plumbing and the automatic switching unit are shown schematically in Fig. 2. The automatic switching unit consisted of ten electromagnetic 3/2-way valves (Fig. 2) and was operated by a PC using a software for measuring technology (ProfiLabExpert 4.0, Abacom, Germany). The operating software controlled the valve positions using two USB relay boards (Abacom, Germany). When switching the valves to a new position, the operating software additionally sent a 1 s long rectangular trigger pulse with 5 V DC to one of the Delta Ray analyzer's two different analogue input channels. One of these channels was used when a target gas measurement had to be started, while a trigger pulse at the other input channel initialized the height measurements. After the Delta Ray analyzer received one of the trigger pulses, the tubes and the measurement cell were purged for 60 s before the analyzer took measurements for 80 s. This purging time was used to ensure that the ~~analyzer took physically separated measurements for the different inlets.~~ first measurement after switching contained less than 0.1% of the previously measured sample (c.f. Sect. 3.1.4).

We used poly ethylene (PE) tubes with 6 mm outer diameter and 4 mm inner diameter (Landefeld GmbH, Kassel, Germany) for the plumbing in the switching unit as well as for the nine height inlets. These inlets were additionally equipped with biweekly ~~changed~~ replaced 1.2 μm PTFE membrane filters (Rettberg GmbH, Göttingen, Germany). The tubes for the ~~height inlets~~ nine height inlets (c.f. Fig. 2) were all equally long (50 m) - except ~~the highest height~~ for the highest inlet that had to be extended to 52 m for practical reasons. The equal (or similar) length of the inlet tubes lead to similar flow rates in the tubing system and similar inlet pressures for the analyzer regardless of the valve position. ~~Thus, we~~ This decreased pressure jumps ~~after~~ when switching from one height position to another. We ~~continuously purged all nine height inlet tubes using an additional purging pump to avoid condensation in the tubes (Fig. 2) . Thus, the~~ purged the main tube to reduce the time the air masses spend in the tubing. To avoid condensation, we heated the valve box (at which we expect a pressure drop) and the adjacent tubing. For heating we used self-regulating heating wires (Horst GmbH, Lorsch, Germany) which produce a constant temperature of 65°C. The flow rate in the height inlet tubes was approximately 1.5 slpm for all heights all the time and the major part of the gas flow was directed into the purging pump. In case of the target standard, the tubing was only purged when the target standard was measured. In this case, an overblow opened to enable gas release at approximately 1 slpm (Fig. 2). For the target measurements as well as for the height measurements the analyzer took a sub-sample of the corresponding inlet line with a flow rate of approximately 0.08 slpm. ~~Because condensation could occur especially in the tubes with this small flow rate and at the valves, we heated the valve box and all tubes that were not continuously purged with higher flow rates. For heating we used self-regulating heating wires (Horst GmbH, Lorsch, Germany) that produce a constant temperature of 65°C.~~ The flow in all tubing was laminar with Reynolds numbers below 100.

For ~~the half-hourly performed target standard measurements , the manual measurements of different additional gas tanks and for~~ measurements as well as calibration, we used gas tanks in 50 l steel containers at 150 to 200 bar pressure containing synthetic air, synthetic air with different CO_2 concentrations and pressurized air (Westfalen AG, Gleichen, Germany). ~~For calibration, we additionally used two~~ Additionally, we used three 1 l gas tanks at 10 bar pressure with pure CO_2 at different (known) δ values that were shipped with the Delta Ray analyzer (Air Liquide, Düsseldorf, Germany). ~~All~~ All used CO_2 containing gas tanks ~~that were used for calibration as well as the target gas tank were~~ were measured high precisely for their CO_2 concentration and isotopic composition in ^{13}C and ^{18}O at the Max Planck Institute for Biogeochemistry in Jena. ~~Due to the limited availability of gas tanks with atmospheric (and high precisely measured)~~ There, the CO_2 concentrations were measured with a Picarro CRDS G1301 and the isotopic composition was measured with IRMS linked to VPDB (VPDP-CO_2) by using the multi point scale anchor JRA-S06 (Wendeberg et al., 2013). The pure CO_2 tanks that were used for δ ~~values, the gas tank that was used for accuracy measurements ('PA-tank', c.f. Table 3) was a secondary standard which was measured in the field using an independently calibrated quantum-cascade laser based absorption spectrometer (QCLAS, *Aerodyne Research Inc.*, Boston, USA).~~ calibration were additionally measured for their ^{13}C composition with IRMS at Geoscience Center in Göttingen (Isotope Geology Division, Göttingen University). All known δ-values and concentrations for the gas tanks used in this application can be found in Table 3 with their corresponding uncertainties.

2.6 Instrument characterization measurements

We ~~quantified the Delta Ray analyzer's long term stability under field conditions as well as its precision, accuracy and cell turnover by the following approaches: The analyzers long term stability under field conditions could be quantified by directly analyzing the half hourly performed target measurements described in Sect. 2.5. For further instrumentcharacterization, we carried out additional measurements that~~ carried out additional measurement in the field and in the lab to quantify precision, evaluate the calibration strategy and quantify the instrument's response time and repeatability. These measurements involved changes in the analyzers plumbing. For all measurements that required connecting different gas tanks to the analyzer, ~~the~~ they were either connected directly to the analyzer's internal ports ('Ref1', 'Ref2', 'CRef1' and 'CRef2') or the plumbing was equivalent to the plumbing of the target gas (Fig.2).

1. Lab measurements to quantify precision and evaluate the calibration strategy
    - We measured the Allan deviation by connecting pressurized air at atmospheric ~~delta~~ δ values to the analyzer and took measurements at the analyzer's maximum data acquisition rate of 1 Hz for two hours. ~~Due to limited supply of gas cylinders at ambient delta values at the field site, this experiment was done in the laboratory before the Delta Ray analyzer was transported to the field site. To quantify the Delta Ray analyzer's accuracy, we replaced the target standard with a gas tank with ambient~~
    - We diluted pure CO_2 with synthetic air over a CO_2 concentration range of 200 to 1500 ppm to measure the concentration dependency of the measured (raw) δ ~~values '~~values. This dilution experiment was carried out for three different tanks with pure CO_2 at different δ values. Each gas tank was measured twice. (Used gas tanks: 'ambient', 'bio1' and 'bio2', c.f. Table 3).
    - We measured the concentration c and the isotopic compositions $\delta^{13}C$ and $\delta^{18}O$ of gases with concentrations ranging from (350 to 500 ppm) and isotopic compositions ranging from -37 to -9.7 ‰ for $\delta^{13}C$ and from -35 to -5 ‰ for $\delta^{18}O$. Each of these measurements was performed three times. (Used gas tanks: 'ambient', 'bio1','bio2', 'PA-tank'~~(~~, SA-CO_2-1,SA-CO_2-4, SA-CO_2-6, c.f. Table 3).
    - We carried out repeated measurements of two pure CO_2 gas tanks at different δ values (diluted to different concentrations between 200 and 3000 ppm) as well as measurements of two gas tanks at different CO_2 concentrations (350 and ~~measured this tank for approximately 10 minutes with a measurement frequency of 1 Hz. The cell turnover~~ 500 ppm). These measurements were repeated every six hours for a period of nine days. (Used gas tanks: 'ambient', 'bio', ('SA-CO_2-1 and 'SA-CO_2-6, c.f. Table 3.)'
2. Field measurements to quantify the setup's response time and repeatability
    - The response time of the tubing and the analyzer was measured by using the automatic switching unit (Fig. 2) to switch from ambient air (~~height 1~~height9) to the target standard. We superimposed the measurements of four switching events to observe the adjacent ~~turnover processes.~~ temporal response processes.
    - The analyzer's repeatability under field conditions was quantified by the half hourly target measurements described in Sect. 2.5

2.7 Meteorological measurements

Supplementary to the measurements with the Delta Ray analyzer, the meteorological tower at the field site is equipped with an Eddy Covariance system to measure CO_2 and H_2O_v fluxes as well as latent and sensible heat fluxes. Additional standard meteorological measurements include continuous measurements of short wave and long wave radiation, wind speed and direction, precipitation, air and soil temperature and air and soil humidity (Anthoni et al., 2004).

2.8 Calibration

2.8.1 Instrument internal calibration

The Delta Ray analyzer is equipped with three different ~~instrument-internal calibration routines~~ internal calibration routines (Thermo Fisher Scientific, 2014). We performed these routines at the field site (~~in situ~~*in situ*) each time the analyzer had to be restarted e.g. after power supply failures, instrument issues or when we manually turned off the analyzer for other reasons. All three instrument internal calibration procedures were usually done one day after restarting the analyzer, thus the instrument was in thermal equilibrium during calibration. ~~We used the three analyzer’s internal calibration routines in the following way~~The three different instrument internal calibration procedures are described below:

- **~~Linearity~~ ’Correction of concentration dependency’ (called ’linearity calibration’ in the instrument’s documentation and operational software)**

  This calibration routine evaluates the concentration dependency of δ ~~-value measurements .~~value measurements (Thermo Fisher Scientific, 2014). Mathematically, an experimentally derived correction factor $f_{\text{correct}}(c_{\text{raw}})$ is multiplied with the raw isotopic ratio R (information from the manufacturer, Thermo Fisher Scientific):

  $$R_{\text{c-corrected}} = f_{\text{correct}}(c_{\text{raw}}) \times R_{\text{raw}} \tag{3}$$

  This factor as a function of concentration is determined via a natural spline fit of measurements of a gas tank with constant δ value at different concentrations (information from the manufacturer, Thermo Fisher Scientific). This is implemented by mixing pure CO_2 with CO_2-free air, yielding concentrations between 200 to 3500 ppm. In our setup we used the pure CO_2 with near to ambient δ ~~-values~~ values (tank ’ambient~~CO_2~~’, c.f. Table 3) ~~was automatically mixed with synthetic air to produce gas with constant δ values at different concentrations ranging from approximately 150 to 3500 ppm CO_2~~ and synthetic air for this calibration.

- **’Delta scale calibration’**

  This calibration routine is based on a two-point-calibration of δ values using two tanks of pure CO_2 with different δ values, that are diluted with synthetic air~~(using two~~. For this calibration, we used the pure CO_2 tanks ’ambient~~CO_2~~’ and ’bio~~CO_2~~’, c.f. Table 3~~)~~.

- **’Concentration calibration’**

  This calibration routine performs a two-point-calibration for CO_2 concentration using two gas tanks with different CO_2 concentrations. We performed this measurement simultaneously to the other two calibration routines in the field, but ~~we could improve the accuracy by performing a post-processing concentration calibration~~for one particular calibration on 15^{th} of October, we had to replace it by a post-calibration, described in Sect. 2.8.2.

~~Additionally to these three instrumentinternal calibration procedures, we measured the~~ The instrument’s internal calibration procedure is based on the measurement of these calibration curves after the instrument is started in combination with repeated measurements of a known gas, so called ’referencing’ (see below). As the different calibrations are only performed once after the instrument is restarted, the accuracy and repeatability of measurements is further based on the assumption that, these relationships remain sufficiently constant, and temporal changes are corrected by ’referencing’.

- **’Referencing’**
  This procedure applies an offset correction of the calibrated δ values using a gas with known δ values that is measured at a freely selectable concentration in regular intervals (information from the manufacturer, Thermo Fisher Scientific). In our experimental setup, referencing is carried out every 30 minutes for 80 s after the tubes have been purged for 60 s using the pure CO_2 standard (’ambient~~CO_2~~’, c.f. Table 3) diluted with synthetic air~~at a freely selectable concentration every 30 minutes as a part of our repetitive measurement cycle. This is implemented in the so called referencingin the Delta Ray analyzers software QTEGRA.~~. We chose the reference concentration to be the same as ~~in the~~ the concentration at the highest inlet in the adjacent measurement cycle, because most of the measurement inlets had ~~delta values close to the values measured~~ concentrations close to those at the highest inlet and the temporal variability of the measured concentrations generally decreased with height. Thus, we ~~achieved to perform the referencing~~ performed the ’referencing’ as close as possible to as many height measurements as possible by using these settings.

Thus, the calibration procedure for δ values can be expressed with the following formula with the correction factor $f_{\mathrm{correct}}(c_{\mathrm{raw}})$ as determined from the concentration dependency correction, and the slope $m_{\delta\mathrm{scale}}$ derived from the δ scale calibration (information from the manufacturer, Thermo Fisher Scientific).

$$\delta_{\mathrm{calibrated}}(R_{\mathrm{raw}};c_{\mathrm{raw}};t) = m_{\delta\mathrm{scale}} \times \underbrace{\left(\frac{f_{\mathrm{correct}}(c_{\mathrm{raw}})R_{\mathrm{raw}}}{R_{\mathrm{std}}} - 1\right)}_{\delta_{\mathrm{c-corrected}}(c_{\mathrm{raw}})} + \delta_{\mathrm{Offset}}(t) \tag{4}$$

2.8.2 Post processing for concentration calibration

~~Measurements with five different gas tanks with known CO$_2$-concentrations ranging from 350 to 450 ppm in the field resulted in considerably high deviations of the (instrument-internal in-situ calibrated) concentrations from known concentrations (high precisely measured at the Max Planck Institute for Biogeochemistry in Jena). In average this deviation was 0.8 ± 0.2 ppm. A possible reason for this resulting deviation is the range of the gas tanks we used for the instrument-internal concentration calibration , that was approximately 300 to 430 ppm. As the half-hourly performed measurement of the target standard(’SACO2-tank’ c.f. Table 3~~For the time period from the 15th of October to 15th of November, we replaced the instrument’s internal concentration calibration by a manual linear calibration, based on manual measurements with six different gas tanks in the field. This was necessary, because measurements with these different gas tanks (including the target standard) showed a ~~very stable behavior (see Sect. 3.1.3), and in especially no jumps occurred when the analyzer was re-calibrated in the field, we used two of these external measurements of known standards with a wider concentration range (’LS-tank’ with approximately 350 and~~

~~'HS-tank' with approximately 450 ppm CO$_2$, c.f. Table 3) to post-calibrate the measured concentrations using a simple two point calibration. With this calibration procedure, we could reduce the mean deviation of the three remaining measured tanks from the corresponding high precise lab measurements from 0.8 ± 0.2 ppm down to in average 0.3 ± 0.1 ppm.~~ consistent linear relationship between raw and known concentrations, that deviated from the linear relationship that was used in the instrument's internal calibration. Thus, we conclude that during this period there was a problem with the instrument's internal concentration calibration which might be related to gas flow or a leak during this particular concentration calibration.

2.9 Multilayer modeling

To test if the measured variability of the ^{13}C composition of respiration can be partly explained by the variability of the ^{13}C composition of recent assimilates, we used the multilayer model CANVEG to simulate the isotopic composition of assimilated material during our measurement campaign. In particular, we analyzed the correlation of modeled ^{13}C$_{\text{Ass}}$ to net radiation R_n, a driver of photosynthesis and photosynthetic discrimination, during our measurement period in autumn 2015. We further compared the resulting relationship between R_n and ^{13}C$_{\text{Ass}}$ to the observed (time lagged) relationship between R_n and the ^{13}C composition of ecosystem respiration R$^{13}_{\text{eco}}$C, derived from the measured Keeling-Plots, c.f. section 3.2.2. This analysis was performed to test the hypotheses of a link between δ values in assimilated material and respiration. We used the multilayer model CANVEG to calculate the isotopic composition of assimilated material δ^{13}C$_{\text{Ass}}$. CANVEG is a biophysical one-dimensional multilayer canopy model, ~~see e. g. .~~(see e.g. Baldocchi, 1997; Baldocchi and Wilson, 2001). This multilayer model uses hourly meteorological inputs (among others temperature, radiation, vapor pressure deficit, wind velocity and CO$_2$ concentration) as main drivers, as well as site specific parameters (leaf area index, leaf clumping status, canopy height et. al.). Based on these input variables, CANVEG iteratively computes the biosphere-atmosphere exchange of water, carbon dioxide and energy as well as the microclimate within and above the canopy at hourly time steps. The carbon, water and energy modules have been validated for various environmental conditions and forest types, ~~see e. g. .~~(see e.g. Baldocchi et al., 1997, 1999, 2002). In particular, the model has also been applied to an unmanaged beech dominated forest field site in approximately 30 km air-line distance to the measurement site of this study (Knohl and Baldocchi, 2008). The isotope enabled version of this model additionally calculates δ^{13}C$_{ij}$, the ^{13}C composition of CO$_2$ ~~δ^{13}C$_{ij}$~~ for each canopy layer i and each hourly timestep j and the corresponding ^{13}C composition of assimilated material δ^{13}C~~$_{Ass,ij}$~~$_{\text{Ass},ij}$ (Baldocchi and Bowling, 2003). In our application, we set up the model to use 40 equally thick layers i and we used our meteorological measurements at the field site, described in Sect. 2.7, as input variables. We validated the model with Eddy Covariance measurements (Table 4) and used the model to calculate the isotopic composition of assimilated material δ^{13}C~~$_{Ass,ij}$~~$_{\text{Ass},ij}$ for each of the 40 canopy ~~layer~~ layers i and for each hourly time step j. The ^{13}C composition of assimilated material $\delta^{13}C_{\text{Ass}}$ on daily timescale was calculated as an assimilation weighted sum over all layers and time steps, with the modeled assimilation rate A_{ij} as a weighting factor:

$$\delta^{13}\text{C}_{\text{Ass}} = \frac{\sum_{i=1}^{40}\sum_{j=1}^{24} A_{ij} \cdot \delta^{13}\text{C}_{\text{Ass},ij}}{\sum_{i=1}^{40}\sum_{j=1}^{24} A_{ij}} \tag{5}$$

We included only hours j and layers i during photosynthesis (with positive assimilation rates). ~~We analyzed the correlation of modeled $\delta^{13}C_{\text{Ass}}$ to net radiation R_n, a driver of photosynthesis and photosynthetic discrimination, during our measurement~~

~~period in autumn 2015. We further compared the resulting relationship between R_n and $\delta^{13}C_{\text{Ass}}$ to the observed relationship between R_n and the ^{13}C composition of respiration R^{13}_{eco}C, derived from the measured Keeling-Plots.~~

3 Results and discussion

3.1 Instrument characteristics

3.1.1 Precision

We use the Allan deviation σ_A at different averaging times τ (Table 5) to characterize the Delta Ray IRIS analyzer's precision. Starting at an averaging time of 1 s, that corresponds to the ~~IRIS analyzers~~ analyzer's maximum data acquisition frequency, the Allan deviation σ_A decreased with $\tau^{-1/2}$ (Fig. 3). This matches the expected behavior of a system that is dominated by white frequency noise. The measured Allan deviation σ_A followed this slope up to averaging times for approximately 300 s for δ value measurements and approximately 200 s for concentration measurements. At these timescales the analyzer showed its maximum precision of 0.02 ‰ VPDB for δ^{13}C, 0.03 ‰ ~~VPDB-CO2~~ VPDB-CO_2 for δ^{18}O and 0.007 ppm for CO_2 concentration. For averaging times above 200-300 s other error sources (such as instrument drift) became significant. For δ^{13}C, the precision of an earlier version of the instrument has also been measured by Geldern et al. (2014), reporting a minimum of σ_A at around 0.04 ‰ for an averaging time of $\tau \approx 550$ s. At this averaging time, we measured ~~an~~ a comparable (slightly better) Allan Deviation below 0.03 ‰ (c.f. Table 5).

Two other averaging times are particularly interesting for our application: Firstly, ~~we chose an~~ the averaging period of 20 s ~~that~~ yields Allan variances below 0.1 ‰ for both δ values and 0.02 ppm for CO_2 concentration~~to solve the trade-off between higher precision and a larger number of measurements~~. Secondly we set the IRIS analyzer's internal referencing procedure (described in Sect. 2.8) to 1800 s which corresponds to an Allan variance of 0.03 ‰ for ~~both δ~~ δ^{13}C and 0.08 ‰ for δ^{18}O values and 0.01 ppm for CO_2 concentration.

3.1.2 ~~Accuracy~~Evaluation of the calibration strategy

The instrument's ~~accuracy was defined as the mean deviation of N=300 field measurements of a tank with pressurized air ('PA-tank', c. f. Table 3) from its known (independently measured) values. The frequency distribution for these measurements is~~ internal calibration strategy (described in section 2.8) is based on:

- A nonlinear relationship between raw δ values and concentrations (Fig. 4).
- A linear relationship between calibrated δ value (measured with IRMS) and the concentration-corrected δ value - $\delta_{c-\text{corrected}}$ in Eq. 4 (Fig. 5, middle and right panel).
- A linear relationship between measured (raw) and real concentrations (Fig. 5, left panel).

- The repeatability of the calibration curves – for δ values modulo the Offset correction, that is applied by the instrument's internal 'referencing' (Fig.6 and Table 7).

Raw δ values show a nonlinear dependency from raw concentrations (Fig. 4). This nonlinear relationship deviates from the concentration-dependency correction applied by the instrument, $\delta_{c-\mathrm{corrected}}(c_{\mathrm{raw}})$ in Eq. 4, as shown in Fig. ~~??) . The so defined accuracy was below 0.1~~4. Here, the instrument internal concentration-dependency correction is shown for the used gas tank 'ambient' after an Offset correction at a concentration of 400 ppm, which is similar to the instrument's internal 'referencing'. Thus, the meam deviations of the measured δ values from the concentration-dependency correction (top panel of Fig.4) give an estimate of the uncertainty of measurements that is related to the deviation from the reference concentration. For referencing at 400 ppm, these deviations were approximately below 0.2 ~~VPDB for δ^{13}C, 0.6~~‰ for ^{13}C and 0.4 ~~for δ^{18}Oand 0.45~~‰ for ^{18}O.

The measured linear relationships for concentration and δ scale calibration (Fig. 5) have R^2 values of above 0.9999 for concentrations, above 0.999 for $\delta\ ^{13}$C, and above 0.998 for $\delta\ ^{18}$O. The linearity and potential accuracy, as defined by Tuzson et al. (2008), can be quantified as the 1 σ standard deviation from the linear fits. The so defined potential accuracy of the instrument internal linear calibrations is 0.45 ppm for CO_2 concentration~~. To evaluate this measured accuracy, we compare it to the setup-dependent expected uncertainty which we define as the sum of the uncertainties of the calibration tanks ('bio CO_2' and 'ambient CO_2' for~~ , 0.24 ‰ for δ^{13}C and 0.3 ‰ for δ^{18}O. For both δ values, this is comparable to the uncertainty related to the nonlinear concentration calibration that varies with δ and c as discussed above.

The repeatability of the calibration curves is discussed here based on measurements of the nonlinear concentration dependency (Fig. 4), and repeated measurements of gas tanks with two different c and δ values ~~'LS-tank' and 'HS-tank' for concentration)and the uncertainty of the pressurized air tank used for the accuracy test 'PA-tank' (Table 3) . The so defined expected uncertainty sums up to approximately~~ to evaluate temporal changes in the respective linear relationships (Fig. 5). These measurements were taken every six hours for a period of nine days. For these repeated measurements the standard deviation of the calibrated values was below 0.2 ppm for concentrations and (if delta values were measured at 400 ~~VPDB for δ^{13}C, 0.7~~ppm and referenced at 380 ~~for δ^{18}O and 0.3~~ppm) below 0.05 and 0.1 ~~ppm for CO_2 concentration. Thus the measured uncertainty was below the expected uncertainty in the case of δ^{13}~~‰ for ^{13}C and ~~δ^{18}O, but it was higher than the expected uncertainty for concentration measurements . In the case of δ^{18}O this is remarkable because the corresponding calibration tanks spanned only a range of -17.5~~^{18}O respectively. Thus, the uncertainty related to the repeatability of the linear calibrations is smaller than the potential accuracy discussed above. For δ values, these values are comparable to the repeatability reported by several authors measured with other laser spectrometers (e.g. Sturm et al., 2012, 2013; Vogel et al., 2013). For concentrations on the other hand, Sturm et al. (2013) reported a much smaller value of 0.03 ~~to -27.2~~ppm, based on more frequent calibration. In our setup, the concentration calibration is only performed once after the instrument is restarted, thus there might be a potential for better repeatability in concentration measurements with more frequent concentration calibration. For δ values measured at concentrations that deviate further from the reference concentration (here 380 ppm), also the repeatability depends on concentration (Table 7). Repeated measurements of these deviations have standard deviations of below 0.15 ‰ for both δ values for concentrations between 200 and 1600 ppm.

For concentration measurements, the uncertainty related to the linear calibration dominates the overall uncertainty, whereas the uncertainty of δ-values measurements depends on the setup, in particular on the 'referencing'. If measurements were carried out at the concentration used during 'referencing', the accuracy is limited by the linear calibrations and the corresponding repeatability (c.f Table 6). If measurements are carried out at concentrations that deviate from the 'referencing' concentration, the accuracy is limited by the actual concentration dependency that deviates from the instrument internal correction of concentration dependency (c.f. Fig. 4 and Table 6). In this case, the accuracy could be further improved by applying a correction of the concentration dependency based on more points. ~~Table 3), whereas the pressurized air used here 'PA-tank' had δ^{18}O value of -5.3 . In the case of CO_2 concentrationthe observed deviation from the expected accuracy might arise from the simple two point calibration we had to perform in a post processing step due to practical limitations (see Sect.2.8.2). Considering these limitations of our calibration setup the measured accuracy seems reasonable to reflect the accuracy of our long-term set up under field conditions.~~

3.1.3 ~~Long-term stability~~Repeatability during the field campaign

We analyzed the ~~long-term stability~~ repeatability of the Delta Ray analyzer under field conditions by evaluating half-hourly measurements of the same gas tank (~~SA-CO2-5~~SA-CO_2-5) during the whole measurement period. We use the standard deviations ~~and mean drift extrapolated to a period of 100 days to quantify the long term stability~~ of measured concentrations and delta values to quantify the repeatability of our set up in the field including our calibration strategy. The standard deviations of these long-term measurements were below ~~0.2~~0.3 ppm for CO_2 concentration~~and below 0.3~~, below 0.2 ‰ for ~~both δ values~~ δ^{13}C and below 0.25 ‰ for δ^{18}O (frequency distributions and time series of the long term measurements are shown with color-coded metadata in Fig. 7.~~The instrument drift, a measure for the instrument's long-term stability, was below 0.04 ‰/100 d for δ^{13}C ,~~[2] For concentrations, the measured repeatability of approximately 0.3 ~~‰~~ppm is slightly larger than the repeatability of the concentration calibration discussed above, but still below the potential accuracy discussed in section 3.1.2. In the case of δ values, the obtained repeatability of approximately 0.2 ~~/100 d for δ^{18}O~~ ‰ for ^{13}C and ~~0.3~~0.25 ~~ppm~~‰ for ^{18}O is larger than the repeatability of the linear calibration parameters obtained during lab measurements (0.05 ~~/100~~‰ for ^{13}C and 0.1 ~~d for CO_2-concentration. Thus, the long term stability measured here is comparable to the measured accuracy of our set up, described in the preceding paragraph~~‰ for ^{18}O). The measured repeatability during the field campaign also exceeds the repeatability of the measurements of the concentration dependency (below 0.15 ‰ for both δ values over a large concentration range) c.f. section 3.1.2. This could be related to the fact, that the δ values of our target standard were out of the calibration range, leading to an enhancement of fluctuations in the calibration parameters.

---

[2] In the case of ^{13}C , we excluded the target measurements between 23^{rd} of September till 29^{th} of September, because we obtained a problem with the ^{13}C calibration that lead to a large jump in the δ ^{13}C value of the (very depleted) target standard. This jump did not occur in the height measurements, probably because they were much closer to the reference δ value.

3.1.4 ~~Turnover~~ Response time

We measured the ~~turnover behavior~~ response time of our system (tubing and measurement cell of the Delta Ray ~~IRIS~~analyzer) by using the valve system shown in Fig. 2 to switch from ambient air with δ^{13}C≈-9 ‰ and δ^{18}O≈1 ‰ to tank air with δ^{13}C≈-38 ‰ and δ^{18}O≈-36 ‰. The time series of the measured δ-values after the change of the valve position (Fig. 8) consisted of three different phases that can be related to different physical processes~~, shown in Fig. 8~~: Within a first phase~~of turnover~~, the measured δ-values remained constant for τ_1 ≈14 s. This is the setup ~~specific-time~~ specific time it took for the gas to flush the tubes and valves before entering the cell. As a second phase~~of turnover, we measured~~ , we observed a quadratic decay of the measured δ-values, which we ~~can~~ relate to mixing of gas within the tubes (before it enters the cell). This phase dominated the ~~turnover~~ temporal response of our system for τ_2 ≈4.5 s. The third phase of ~~turnover~~ temporal response is the exponential decay with a characteristic decay time (defined here using the 10 %-threshold) $\tau_{10\%} \approx 10$ s for δ^{13}C and $\tau_{10\%} \approx 11$ s for δ^{18}O. This exponential behavior can be derived for an idealized situation that includes perfect mixing in a volume V_{mix} yielding:

$$\tau_{10\%} = \frac{log(10) \cdot p_{\mathrm{cell}} \cdot V_{\mathrm{mix}}}{\Phi}$$

With flow rate Φ, cell pressure p_{cell} and effective mixing volume V_{mix}. Using the volume of the measurement cell as an upper threshold for the effective mixing volume within the cell: $\max(V_{\mathrm{mix}}) = V_{\mathrm{cell}} = 80$ ml, we can calculate an upper threshold for $\tau_{10\%}$. With the instruments flow rate of $\Phi = 0.08$ slpm and the cell pressure of $p_{\mathrm{cell}} \approx 100$ mbar we get $\tau_{10\%,\mathrm{max}} \approx 13.6$ s. Thus the measured value of ~~$\tau_{10\%,\mathrm{max}}$~~ $\tau_{10\%}$ is slightly below this value, indicating $V_{\mathrm{mix}} < V_{\mathrm{cell}}$. We define the total ~~turnover~~ response time τ_{tot} as the time-span it took until the step change between the two inlets reached 0.1 % of the corresponding difference in δ values, with $\tau_3 = \tau_{0.1\%} = 3 \cdot \tau_{10\%}$. The three different phases of ~~turnover~~ instrument response (tube transport τ_1, tube mixing dominated change τ_2 and cell mixing dominated change τ_3) summed up to a net ~~turnover~~ response time $\tau_{\mathrm{tot}} = \tau_1 + \tau_2 + \tau_3 <$ 60 s. Thus, the cell flushing time of our application (60 s) is appropriate to produce independent measurements of two different inlets.

3.1.5 Utilization rate, power consumption and maintenance effort

We define the utilization rate as the number of successfully recorded measurement cycles divided by the number of measurement cycles that were theoretically possible during the field campaign (approximately 4200). This can be calculated separately for a) profile measurements and b) target gas measurements, because some data gaps were specific for target measurements. The utilization rate for was approximately 80 % for measurements of the height profile and approximately 70 % for target gas measurements. Two major reasons for data gaps reduced the utilization rate for both, profile and target measurement by ~~5~~8.6 % (a laser alignment problem that ~~could be resolved after 4~~ was resolved after 7 days) and 6 % (three data acquisition problems, the longest lasting three days). Additionally, four external power supply problems at the field site lead to a further reduction of the utilization rate by 3.3 %. These data gaps, as well as smaller datagaps, that reduced the utilization rate are listed in Table 8. In ~~the~~ case of target measurements, the main reason for data gaps (accounting for a reduction of utilization rate of more than 9 %) were plumbing issues that lead to a contamination of the target gas by ambient air. Thus a more stable target plumbing would be a promising approach to increase the utilization rate, as well as a more stable power supply and more frequent field trips.

Maintenance effort and power consumption of the whole setup were moderate: The analyzer's power consumption of approximately 220 W was slightly smaller than the power consumption of the basic infrastructure of the setup that included the pump to purge the nine inlet tubes and the heated valve box ~~and its controlling unit (see Table ??~~(330 W). To maintain and to control the setup, we went to the field site weekly or biweekly and used remote access to the instrument via a satellite connection.

3.2 Ecological Application

3.2.1 Time series of measured quantities

The measured CO_2 concentrations in 45 m height at our field site in a managed beech forest in Central Germany ranged from 385 to 450 ppm with corresponding δ values between -11 to -7 ‰ for ^{13}C and between -6 and 2 ‰ for ^{18}O over a three-month period in autumn 2015 (Fig. 9). As the lower heights commonly contain larger amounts of respired ~~(typically lighter)~~ CO_2 with a typically lighter carbon and oxygen composition, the lower inlets show larger CO_2 concentrations c with smaller δ values. We calculated a three-month time series of nighttime Keeling-Plot intercepts $\delta^{13}\mathrm{C}_{\mathrm{KP}}$ and $\delta^{18}\mathrm{O}_{\mathrm{KP}}$~~(shown with temperature and precipitation data in Fig. 10)~~, that can be interpreted as the respective isotopic composition of ~~ecosystem respiration~~ nighttime net ecosystem CO_2 exchange (respiration) R^{13}_{eco}C and R^{18}_{eco}O ~~.~~ (shown with temperature and precipitation data in Fig. 10). A particular feature of the measurement period is an early snow and frost event with negative temperatures during four nights between 11. and 15. October 2015 (Fig. 10). The corresponding snow event on ~~13. October could be identified~~ 13th of October was visible on a canopy picture, taken at midday on 13. October 2015. The time of the snow and frost event coincided with changes in the characteristics of δ^{18}O, R^{18}_{eco}O and R^{13}_{eco}C: For δ^{18}O and R^{18}_{eco}O a strong decrease was obtained after the snow event. This decrease was the largest signal in the respective time series. For R^{13}_{eco}C, the analysis of its potential meteorological drivers yielded different results for the time periods before and after the first snow. Additionally, according to Eddy Covariance measurements, the forest was a net CO_2 sink with negative diurnal net ecosystem exchange (NEE) before the 12. October (with only one exception), whereas it was a net CO_2 source with positive diurnal NEE after the snow event on 13. October (also with only one exception).

3.2.2 Potential drivers for R^{13}_{eco}C

Previous studies linked the temporal variability of the ^{13}C composition of ecosystem respiration R^{13}_{eco}C partially to changes in the meteorological conditions during photosynthesis, namely relative humidity RH, Vapor pressure deficit VPD, photosynthetically active radiation (PAR) and the ratio VPD/PAR (Ekblad and Högberg, 2001; Bowling et al., 2002; Knohl et al., 2005). These links occurred with time lags ~~,~~ that correspond to the time lag between assimilation and respiration, which is approximately four to five days for mature trees (Kuzyakov and Gavrichkova, 2010). The observed time lagged links between meteorological variables and R^{13}_{eco}C were interpreted by the respective authors as an indication for a link between the isotopic composition of respiration $R^{13}_{\mathrm{eco}}\mathrm{C}$ ~~to~~ and the isotopic composition of recent assimilates $\delta^{13}\mathrm{C}_{\mathrm{Ass}}$, which is controlled by photosynthetic discrimination of the heavier ^{13}C according to the Farquhar Model (Farquhar et al., 1989). Thus, in accordance with previous studies, we hypothesize that:

Hypothesis (a): The variability of $R^{13}_{\mathrm{eco}}\mathrm{C}$ can be partly explained by the isotopic composition of recent assimilates $\delta^{13}\mathrm{C}_{\mathrm{Ass}}$, which is controlled by meteorological drivers during photosynthesis according to the Farquhar model. Thus, the variability of $R^{13}_{\mathrm{eco}}\mathrm{C}$ ~~can be~~ is linked to the variability of meteorological drivers of photosynthesis and photosynthetic discrimination with a time lag that is consistent with the time lag between respiration and assimilation.

To test this hypothesis, we calculated the Pearson correlation coefficient r_{pear} between $R^{13}_{\mathrm{eco}}\mathrm{C}$ and the n-day sum (with n from 1 to 6) of the meteorological quantities that we expect to control ^{13}C discrimination for different time shifts τ. For the time period before the first snow (when the ecosystem was a $\mathrm{CO_2}$ sink), the strongest correlation we found was a moderate negative correlation between $R^{13}_{\mathrm{eco}}\mathrm{C}$ and the two-day-sum of net radiation R_n with a time shift τ of two days (Fig. 11). This correlation is significant with a Pearson correlation coefficient r_{pear} of approximately ~~-0.55~~ -0.56, which is clearly beyond the corresponding critical value of approximately ± 0.38 for N=~~46~~ 45 and $\alpha = 0.005$. The time lag of this correlation is in accordance with the expected time lag between assimilation and respiration of two to five days for mature trees (Kuzyakov and Gavrichkova, 2010). But the correlation itself cannot be directly explained by the Farquhar model of discrimination as radiation influences both, the $\mathrm{CO_2}$ supply (by influencing stomatal conductance) and the $\mathrm{CO_2}$ demand (by influencing assimilation) in the leaf (Farquhar and Sharkey, 1982). In particular we did not find a significant time lagged positive correlation between $R^{13}_{\mathrm{eco}}\mathrm{C}$ and VPD, RH or the ratio VPD/PAR (Fig. 11), which could be directly associated with the Farquhar Model and ~~has~~ have been found by the above mentioned studies. To test if it might be still reasonable to interpret the observed negative correlation of $R^{13}_{\mathrm{eco}}\mathrm{C}$ with R_n as a time lagged link between $R^{13}_{\mathrm{eco}}\mathrm{C}$ and isotopic composition of recently assimilated material $\delta^{13}\mathrm{C}_{\mathrm{Ass}}$ on ecosystem scale, we performed a more complex calculation of $\delta^{13}\mathrm{C}_{\mathrm{Ass}}$ by using the multilayer model CANVEG, c.f. Sect. 2.9. ~~During the~~ The advantage of CANVEG is that it accounts for the non-linear interactions between air temperature, air humidity, radiation, stomatal conductance and photosynthesis. Before the first snow event during our measurement period, the modeled $\delta^{13}\mathrm{C}_{\mathrm{Ass}}$ correlated significantly ~~to~~ with the diurnal sum of net radiation R_n with an r_{pear} of 0.89 (Fig. 12) - corresponding $r_{\mathrm{crit}} \approx 0.33$ for N=63. But in contrast to the time lagged correlation, which we found in our Keeling-Plot data, this correlation is positive (Fig. 12). As the multilayer model does not support the interpretation of the observed negative correlation between R_n and $R^{13}_{\mathrm{eco}}\mathrm{C}$ through the variability of the isotopic composition of recent assimilates $\delta^{13}\mathrm{C}_{\mathrm{Ass}}$, it does not support hypothesis (a).

An alternative interpretation of the observed correlation between the isotopic composition of respiration $R^{13}_{\mathrm{eco}}\mathrm{C}$ and net radiation R_n would be a link between $R^{13}_{\mathrm{eco}}\mathrm{C}$ and the amount of recent assimilates (alternatively to the isotopic composition of recent assimilates). ~~As~~ Because soil respiration has been measured to account for around 80~~% of total~~ % of ecosystem respiration in an old beech forest in below 30 km distance to our field site (Knohl et al., 2008), we assume that soil respiration dominates ecosystem respiration and thus we further focus on soil respiration and discuss the following hypothesis:

Hypothesis (b): The observed time-lagged correlation between R_{eco}^{13}C and net radiation R_n is ~~not related to differences in discrimination, but rather to differences in the~~ related to the temporal variability of the ratio of autotrophic to total soil respiration[3].

A link between photosynthesis and autotrophic soil respiration has been shown in many studies throughout different ecosystems, including a beech dominated forest in less than 30 km air-line distance to our field site in a managed beech forest (Moyano et al., 2008). In this study, the authors found that 73 % of the variability in rhizosphere respiration (the major part of autotrophic soil respiration) correlated with photosynthesis (GPP) and the ratio between autotrophic and total soil respiration was approximately 50 %. Additionally, evidences for a large temporal variability on diurnal and seasonal scale of the contribution of autotrophic to total soil respiration have been reported for a temperate hardwood forest (Savage et al., 2013) and for a mature temperate boreal forest (Carbone et al., 2016). In our field experiment, the observed correlation between R_{eco}^{13}C and R_n with an r_{pear} of ~~0.55~~ 0.56 (and thus ($r_{\mathrm{pear}}^2 = 0.3$) links 30 % of the variability of R_{eco}^{13}C to R_n with a time lag of 2-4 days. As the measured isotopic composition of ecosystem respiration R_{eco}^{13}C spanned a range of 6 ‰, this corresponds to a range of 1.8 %. Hypothesis (b) would further imply, that this variability over a range of 1.8 ‰ corresponds to that proportion of the variability of autotrophic respiration that is linked to photosynthesis. If we estimate this proportion to represent 73 % of the total variability of autotrophic respiration (following Moyano et al., 2008), the corresponding total variability of autotrophic respiration would correspond to a range of approximately 2.5 ‰ . If in autumn the ratio of autotrophic to total respiration would approximate 0 %, this value of 2.5 ‰ would be equal to the difference $\Delta_{\mathrm{tot-aut}} = \delta_{\mathrm{tot}} - \delta_{\mathrm{aut}}$ between the isotopic composition of total respiration δ_{tot} and the isotopic composition of autotrophic respiration δ_{aut}. In general, a value of $\Delta_{\mathrm{tot-aut}} = +2.5$‰ is within the range of differences, that have been reviewed to be ~~in~~ on average about +4 ‰ (Bowling et al., 2008) for different ecosystems. A positive value of $\Delta_{\mathrm{tot-aut}}$ with a lighter ~~isotopic~~ δ^{13}C composition of autotrophic respiration would be consistent to Hypothesis (b). As a note of caution, however, none of the studies that analyze autotrophic soil respiration in the above mentioned review, was performed in a forest ecosystem. For C3 woody species, including forests, more enriched ~~isotopic compositions~~ δ^{13}C values of autotrophic soil respiration, and thus negative values for $\Delta_{\mathrm{tot-aut}}$, have been reported (Ghashghaie and Badeck, 2014). In a beech forest in Southern Germany, the sign of some involved fractionation effects varied temporally (Paya et al., 2016). Thus, the comparison with literature data about the temporal variability of the ratio between autotrophic and total soil respiration and the respective isotopic compositions gives the possibility that hypothesis (b) is true, but we can, however, not prove it without additional independent measurements. To test this hypothesis, we would need to measure the amount and the isotopic composition of autotrophic respiration, total soil respiration and ecosystem respiration (e.g. by a trenching experiment) at our field site with an appropriate time resolution to capture the day-to-day variability during the field campaign. Lab measurements using incubations could also give an idea of the isotopic composition of autotrophic and total soil respiration, but would not fully reflect field site conditions.

---

[3] The term 'autotrophic' is not consistently defined among different authors. Here we use this term equivalent to 'root derived respiration', including respiration from the living root tissue, from micro-organisms in the rhizosphere and mycorrrhizal symbiotic funghi.

3.2.3 Characteristics of R^{18}_{eco}O and δ^{18}O

The seasonal variability of δ^{18}O and R^{18}_{eco}O (shown in Fig. 9 and Fig. 10) are influenced by oxygen exchange when CO_2 gets dissolved in different water pools (e.g. leaf and soil water) with variable isotopic compositions. These isotopic compositions in turn, are controlled by multiple physical and biological factors such as temperature, precipitation, vapor pressure deficit (VPD) or the activity of the enzyme carbonic anhydrase, that accelerates the oxygen exchange between water and CO_2, (Miller et al., 1999; Farquhar et al., 1993; Gillon and Yakir, 2000; Bowling et al., 2003a; Wingate et al., 2009). The strongest feature of the measured time series of R^{18}_{eco}O is an approximately 30 ‰ large decrease within ten days from approximately ~~-15~~-18 ‰ on ~~8.~~7. October to approximately -46 ‰ on 18. October (Fig. 10). During the same time period, the δ^{18}O value of nighttime ambient CO_2 in 45 m height decreased from approximately -1 ‰ down to -3.5 ‰ at nighttime and down to -6 ‰ during daytime (Fig. 9). As for R^{18}_{eco}O, this decrease is the strongest signal in the measured time series of δ^{18}O. The time of these decreases in R^{18}_{eco}O and δ^{18}O coincided with the time of the first snow and frost event in autumn 2015. This indicates that the snow event has a noticeable effect on both δ^{18}O and R^{18}_{eco}O, but as the change in (nighttime) R^{18}_{eco}O is more than ten times larger than the corresponding change in δ^{18}O of nighttime CO_2 this effect is particularly enhanced for R^{18}_{eco}O. For comparison, similar strong peaks in $\mathrm{R}^{18}_{\mathrm{eco}}$O have been observed in a semi-arid woodland after precipitation in New Mexico (Shim et al., 2013), but this study refers to a monsoon dominated ecosystem with comparably large variability in the ^{18}O and does not focus on the difference of these pulses of snow and rain events.

Possible explanations for the observed large decreases in both δ^{18}O and R^{18}_{eco}O after the snow would involve the ^{18}O exchange of CO_2 with water pools that are fed by the recent snow event and the response to changes in multiple of the above mentioned physical and biological factors that influence the oxygen exchange between CO_2 and water. One of the factors that can cause a depletion in ^{18}O due to the exchange of oxygen between CO_2 with snow-fed water pools is the fact that snow has in general a lighter ~~isotopic composition~~ ^{18}O-composition than rain. The isotopic composition of rain can often be related to Rayleigh fractionation processes (Gat, 1996) and thus is related to isotopic exchange between the raindrops and air masses in clouds when rain is falling ~~down~~ (Gat, 1996, citing Bolin, 1959 and Friedman et al., 1962). As a result of the continuous isotopic exchange with air masses in the cloud, raindrops do not carry the very depleted isotopic composition within the cloud whereas for snow, the isotopic exchange between the falling snowflakes and the air masses in the cloud does not take place, resulting in a more depleted precipitation (Gat, 1996). As example, Orlowski et al. (2016) reported a maximal difference of approximately 15.5 ‰ between the δ^{18}O values of rain and snow over a two-year measurement period at a field site in approximately 160 km air-line distance from our field site. A smaller maximal difference of approximately 9 ‰ between the δ^{18}O of snow and the ~~monthly means of the isotopic composition of~~ corresponding monthly means for rain was reported by Wenninger et al. (2011), based on two years of measurements at two catchments in German black forest 414 km air-line distance from our field site. Thus, the ~~depleted~~ ^{18}O-depleted isotopic composition of snow compared to rain ~~can explain a part but probably not all~~ may explain some of the observed 30 ‰ decrease in R^{18}_{eco}O. One possible additional effect could be the fact that soil respired CO_2 is typically in equilibrium not with rain, but with soil water in the top soil layers (0 to 20 cm) (Miller et al., 1999; Wingate et al., 2009). Evaporative effects can shift the isotopic composition in the upper soil layers towards more ^{18}O enriched values (Miller et al., 1999; Wingate et al., 2009) potentially increasing the δ^{18}O difference ~~between~~ before and after the snow event.

We tested the correlation between R^{18}_{eco}O and different meteorological variables that potentially control the isotopic composition of different water pools within the ecosystem over the whole measurement period as well as the sub-periods before and after the first snow (Table 9). As the underlying multiple interaction processes between oxygen in CO_2 and different water pools and the respective isotopic compositions of these pools are complex, this analysis was not performed to causally link the measured R^{18}_{eco}O to a single meteorological driver but rather to look for changes of these correlations that could be interpreted as changes in the processes that drive R^{18}_{eco}O before and after the snow event. For the whole measurement period, the strongest of the analyzed correlations was a correlation between R^{18}_{eco}O and soil moisture at a depth of 8 cm with an R^2 of ~~0.48~~ 0.49 and $p<10^{-9}$. As this correlation becomes insignificant when it is calculated for the periods before and after the snow separately, it can be related to the strong decrease in R^{18}_{eco}O after the snow event that correlates to a rise in soil moisture when the snow melts (Fig. 10). This would be consistent to a heavier ~~isotopic~~ ^{18}O composition in the top soil layers (due to evaporation) before the snow, yielding also higher δ^{18}O values of R^{18}_{eco}O. Also other variables that correlated significantly with R^{18}_{eco}O during the whole measurement period such as soil and air temperatures or shortwave radiation (Table 9) are related to soil evaporation. For the sub-periods before and after the first snow, we found multiple significant correlations with meteorological drivers such as soil and air temperatures, pressure or actual vapor pressure (Table 9). The significant correlations before the first snow become insignificant (or less significant) after the snow and vice versa. This behavior indicates a difference in the processes that drive the ^{18}O isotopic composition of ~~ecosystem respiration~~ nighttime net ecosystem CO_2 exchange R^{18}_{eco}O before and after the snow event.

4 Conclusions

Field-applicable instruments to analyze the isotopic composition of CO_2 have a large potential to be useful for long term measurement setups on meteorological towers and networks such as ICOS https://www.icos-ri.eu/ or NEON http://www.neonscience.org/ to deliver new insights into the carbon cycle. The new Isotope Ratio Infrared Spectrometer (IRIS) Delta Ray used in this study provides an opportunity to measure the CO_2 concentration c and its isotopic compositions δ^{13}C and δ^{18}O with limited maintenance effort at remote sites. Here, we ~~successfully~~ evaluate the instrument internal calibration and demonstrate the field applicability of the Delta Ray IRIS, which we used to measure c, δ^{13}C and δ^{18}O in a managed beech forest for three months in autumn 2015. The Delta Ray IRIS implemented here with the instrument's internal calibration, showed adequate precision, accuracy and ~~long-term stability~~ repeatability to perform robust measurements of c, δ^{13}C and δ^{18}O in air in our continuous setup. For measurements of δ values at concentrations that deviate from the 'referencing' concentration, the uncertainty is dominated by the instrument internal correction of concentration dependency and improvements of the accuracy could potentially be achieved by more detailed analysis of this concentration dependency. The easy operation of the automatically calibrated Delta Ray IRIS allowed us to measure seasonal variability of the isotopic composition of nighttime CO_2 exchange based on Keeling-Plots. The strong effect of the first frost and snow event on both the δ^{13}C and δ^{18}O of nighttime

CO_2 exchange indicates that singular events, even if short, may strongly influence the isotopic imprint of terrestrial ecosystems on atmospheric CO_2.

5 Code availability

An earlier version of the multilayer model CANVEG can be found here:
https://nature.berkeley.edu/biometlab/BiometWeb/canoak_V2.c

6 Data availability

All data used for the figures presented here is provided in the supplementary material.

7 Appendices

- Appendix A: Measures to improve data quality

Author contributions. The authors contributed to this paper in the following ways: The experimental setup in the field and data processing were carried out, discussed and interpreted by Jelka Braden-Behrens and Alexander Knohl. The validation of and simulations with the multilayer model CANVEG (Sect. 2.9) were performed, discussed and interpreted by Yuan Yan, Jelka Braden-Behrens and Alexander Knohl. All authors proof-read and commented on the paper.

8 Competing interests

We declare that we have no conflict of interest. However, we borrowed the instrument at no cost from *Thermo Scientific*, Waltham, USA, to perform instrument tests and to use the instrument under field conditions~~and~~. Additionally we could do lab measurements to evaluate the calibration strategy at the facility of Thermo Scientific in Bremen at no cost. Jelka Braden-Behrens and Alexander Knohl published a short (not peer reviewed) technical paper (Braden-Behrens et al., 2017) together with HJ Jost and Magda Mandic, who were both working for *Thermo Scientific*, when we borrowed the instrument. This not peer reviewed technical paper also briefly describes our experimental setup and discusses instrument performance.

Acknowledgements. This project was partly funded by the Dorothea-Schlözer-Fellowship and by the German Research Foundation (DFG, project ISOFLUXES KN 582/7-1). The work was partially supported by the European Research Council under the European Union's Horizon 2020 research and innovation programme (grant agreement n. 682512 – OXYFLUX). We thank *Thermo Scientific*, Waltham, USA, to borrow us the instrument for free and ~~in particular HJ Jostand Magda Mandic~~ made it possible for us to do additional measurements in the lab. We particularly thank HJ Jost, Magda Mandic and Danijela Smajgl for their advice and support especially concerning how to set up, calibrate and operate the Delta Ray analyzer. The technicians of the bioclimatology group of the University of Goettingen, especially Dietmar Fellert

Frank Tiedemann and Edgar Tunsch as well as the student assistant Elke Schäpermeier helped substantially with the experimental setup and maintenance. We thank Yakov Kuzyakov, Lydia Gentsch and Mattia Bonazza for their remarks on data interpretation. Additionally we thank the forest manager Ulrich Breitenstein for allowing the experimental setup at this site.

References

Affek, H. and Yakir, D.: The stable isotopic composition of atmospheric CO_2, in: Treatise on geochemistry, edited by Holland, H. and Turekian, K., vol. 5, chap. 5.7, pp. 179–212, Elsevier, 2 edn., doi:10.1016/B978-0-08-095975-7.00407-1, 2014.

Anthoni, P., Knohl, A., Rebmann, C., Freibauer, A., Mund, M., Ziegler, W., Kolle, O., and Schulze, E. D.: Forest and agricultural land-use-dependent CO_2 exchange in Thuringia, Germany, Glob. Change Biol., 10, 2005–2019, doi:10.1111/j.1365-2486.2004.00863.x, 2004.

Baldocchi, D. D.: Measuring and modelling carbon dioxide and water vapour exchange over a temperate broad-leaved forest during the 1995 summer drought, Plant, Cell Environ., 20, 1108–1122, doi:10.1046/j.1365-3040.1997.d01-147.x, 1997.

Baldocchi, D. D. and Bowling, D. R.: Modelling the discrimination of $^{13}CO_2$ above and within a temperate broad-leaved forest canopy on hourly to seasonal time scales, Plant, Cell Environ., 26, 231–244, doi:10.1046/j.1365-3040.2003.00953.x, 2003.

Baldocchi, D. D. and Wilson, K. B.: Modelling CO_2 and water vapor exchange of a temperate broadleaved forest across hourly to decadal time scales, Ecol. Model., 142, 155–184, doi:10.1016/S0304-3800(01)00287-3, 2001.

Baldocchi, D. D., Vogel, C. A., and Hall, B.: Seasonal variation of carbon dioxide exchange rates above and below a boreal jack pine forest, Agr. Forest Meteorol., 83, 147–170, doi:10.1016/S0168-1923(96)02335-0, 1997.

Baldocchi, D. D., Fuentes, J. D., Bowling, D. R., Turnipseed, A. A., and Monson, R. K.: Scaling isoprene fluxes from leaves to canopies: Test cases over a boreal aspen and a mixed species temperate forest, J. Appl. Meteorol., 38, 885–898, doi:10.1175/1520-0450(1999)038<0885:SIFFLT>2.0.CO;2, 1999.

Baldocchi, D. D., Wilson, K. B., and Gu, L.: How the environment, canopy structure and canopy physiological functioning influence carbon, water and energy fluxes of a temperate broad-leaved deciduous forest - An assessment with the biophysical model CANOAK., Tree Physiol., 22, 1065–1077, doi:10.1093/treephys/22.15-16.1065, 2002.

Ballantyne, A. P., Miller, J. B., Baker, I. T., Tans, P. P., and White, J. W. C.: Novel applications of carbon isotopes in atmospheric CO_2: What can atmospheric measurements teach us about processes in the biosphere?, Biogeosciences, 8, 3093–3106, doi:10.5194/bg-8-3093-2011, 2011.

Barbour, M. M., Hunt, J. E., Kodama, N., Laubach, J., McSeveny, T. M., Rogers, G. N. D., Tcherkez, G., and Wingate, L.: Rapid changes in $\delta^{13}C$ of ecosystem-respired CO_2 after sunset are consistent with transient ^{13}C enrichment of leaf respired CO_2, New Phytol., 190, 990–1002, doi:10.1111/j.1469-8137.2010.03635.x, 2011.

Bolin, B.: On the use of tritium as a tracer for water in nature, in: Proceedings of the 2nd conference on the peaceful uses of atomic energy, pp. 18:336–44, UN, Geneva, 1959.

Bowling, D. R., Tans, P. P., and Monson, R. K.: Partitioning net ecosystem carbon exchange with isotopic fluxes of CO_2, Glob. Change Biol., 7, 127–145, doi:10.1046/j.1365-2486.2001.00400.x, 2001.

Bowling, D. R., McDowell, N. G., Bond, B. J., Law, B. E., and Ehleringer, J. R.: ^{13}C content of ecosystem respiration is linked to precipitation and vapor pressure deficit, Oecologia, 131, 113–124, doi:10.1007/s00442-001-0851-y, 2002.

Bowling, D. R., McDowell, N. G., Welker, J. M., Bond, B. J., Law, B. E., and Ehleringer, J. R.: Oxygen isotope content of CO_2 in nocturnal ecosystem respiration: 2. Short-term dynamics of foliar and soil component fluxes in an old-growth ponderosa pine forest, Global Biogeochem. Cy., 17, GB2082, doi:10.1029/2003GB002082, 2003a.

Bowling, D. R., McDowell, N. G., Welker, J. M., Bond, B. J., Law, B. E., and Ehleringer, J. R.: Oxygen isotope content of CO_2 in nocturnal ecosystem respiration: 1. Observations in forests along a precipitation transect in Oregon, USA, Global Biogeochem. Cy., 17, 3101–3114, doi:10.1029/2003GB002081, 2003b.

Bowling, D. R., Sargent, S. D., Tanner, B. D., and Ehleringer, J. R.: Tunable diode laser absorption spectroscopy for stable isotope studies of ecosystem-atmosphere CO_2 exchange, Agr. Forest Meteorol., 118, 1–19, doi:10.1016/S0168-1923(03)00074-1, 2003c.

Bowling, D. R., Burns, S. P., Conway, T. J., Monson, R. K., and White, J. W. C.: Extensive observations of CO_2 carbon isotope content in and above a high-elevation subalpine forest, Global Biogeochem. Cy., 19, GB3023, doi:10.1029/2004GB002394, 2005.

Bowling, D. R., Pataki, D. E., and Randerson, J. T.: Carbon isotopes in terrestrial ecosystem pools and CO_2 fluxes, New Phytol., 178, 24–40, doi:10.1111/j.1469-8137.2007.02342.x, 2008.

Braden-Behrens, J., Knohl, A., Jost, H.-J., and Mandic, M.: Measuring the isotopic composition of ecosystem respiration in a temperate beech forest, Thermo Sci. White Pap., p. WP30385, http://tools.thermofisher.com/content/sfs/brochures/WP-30385-IRIS-Isotopic-Composition-Respiration-Beech-WP30385-EN.pdf, 2017.

Carbone, M. S., Richardson, A. D., Chen, M., Davidson, E. A., Hughes, H., Savage, K. E., and Hollinger, D. Y.: Constrained partitioning of autotrophic and heterotrophic respiration reduces model uncertainties of forest ecosystem carbon fluxes but not stocks, J. Geophys. Res.-Biogeo., 121, 2476–2492, doi:10.1002/2016JG003386, 2016.

Coplen, T. B.: Guidelines and recommended terms for expression of stable-isotope-ratio and gas-ratio measurement results, Rapid Commun. Mass Sp., 25, 2538–2560, doi:10.1002/rcm.5129, 2011.

Ekblad, A. and Högberg, P.: Natural abundance of ^{13}C in CO_2 respired from forest soils reveals speed of link between tree photosynthesis and root respiration, Oecologia, 127, 305–308, doi:10.1007/s004420100667, 2001.

Esler, M. B., Griffith, D. W. T., Wilson, S. R., and Steele, L. P.: Precision trace gas analysis by FT-IR spectroscopy. 2. The $^{13}C/^{12}C$ isotope ratio of CO_2, Anal. Chem., 72, 216–221, doi:10.1021/ac990563x, 2000.

Farquhar, G. D. and Sharkey, T. D.: Stomatal conductance and photosynthesis, Annu. Rev. Plant Physiol., 33, 317–345, doi:10.1146/annurev.pp.33.060182.001533, 1982.

Farquhar, G. D., Ehleringer, J. R., and Hubick, K. T.: Carbon isotope discrimination and photosynthesis, Annu. Rev. Plant Phys., 40, 503–537, doi:10.1146/annurev.pp.40.060189.002443, 1989.

Farquhar, G. D., Lloyd, J., Taylor, J. A., Flanagan, L. B., Syvertsen, J. P., Hubick, K. T., Wong, S. C., and Ehleringer, J. R.: Vegetation effects on the isotope composition of oxygen in atmospheric CO_2, Nature, 363, 439–443, doi:10.1038/363439a0, 1993.

Flanagan, L. B. and Ehleringer, J. R.: Ecosystem–atmosphere CO_2 exchange: interpreting signals of change using stable isotope ratios, Trends Ecol. Evol., 13, 10–14, doi:10.1016/S0169-5347(97)01275-5, 1998.

Friedman, I., Machta, L., and Soller, R.: Water-vapor exchange between a water droplet and its environment, J. Geophys. Res., 67, 2761–2766, doi:10.1029/JZ067i007p02761, 1962.

Gat, J. R.: Oxygen and hydrogen isotopes in the hydrologic cycle, Annu. Rev. Earth Pl. Sc., 24, 225–262, doi:10.1146/annurev.earth.24.1.225, 1996.

Geldern, R. V., Nowak, M. E., Zimmer, M., Szizybalski, A., Myrttinen, A., Barth, J. A. C., and Jost, H.-J.: Field-based stable isotope analysis of carbon dioxide by mid-infrared laser spectroscopy for carbon capture and storage monitoring, Anal. Chem., 86, 12 191–12 198, doi:10.1021/ac5031732, 2014.

Gemery, P. A., Trolier, M., and White, J. W. C.: Oxygen isotope exchange between carbon dioxide and water following atmospheric sampling using glass flasks, J. Geophys. Res., 101, 14 415–14 420, doi:10.1029/96JD00053, 1996.

Ghashghaie, J. and Badeck, F. W.: Opposite carbon isotope discrimination during dark respiration in leaves versus roots - a review, New Phytol., 201, 751–769, doi:10.1111/nph.12563, 2014.

Gillon, J. S. and Yakir, D.: Naturally low carbonic anhydrase activity in C_4 and C_3 plants limits discrimination against $C^{18}OO$ during photosynthesis, Plant, Cell Environ., 23, 201–213, doi:10.1046/j.1365-3040.2000.00597.x, 2000.

Griffis, T. J.: Tracing the flow of carbon dioxide and water vapor between the biosphere and atmosphere: A review of optical isotope techniques and their application, Agr. Forest Meteorol., 174-175, 85–109, doi:10.1016/j.agrformet.2013.02.009, 2013.

Griffith, D. W. T., Deutscher, N. M., Caldow, C., Kettlewell, G., Riggenbach, M., and Hammer, S.: A Fourier transform infrared trace gas and isotope analyser for atmospheric applications, Atmos. Meas. Tech., 5, 2481–2498, doi:10.5194/amt-5-2481-2012, 2012.

Guillon, S., Pili, E., and Agrinier, P.: Using a laser-based CO_2 carbon isotope analyser to investigate gas transfer in geological media, Appl. Phys. B-Lasers O., 107, 449–457, doi:10.1007/s00340-012-4942-8, 2012.

International Atomic Energy Agency: Reference and intercomparison materials for stable isotopes of light elements, in: Proceedings of a consultants meeting, edited by IAEA, pp. IAEA–TECDOC–825, Vienna, 1995.

Keeling, C. D.: The concentration and isotopic abundances of atmospheric carbon dioxide in rural areas, Geochim. Cosmochim. Ac., 13, 322–334, doi:10.1016/0016-7037(58)90033-4, 1958.

Kerstel, E. and Gianfrani, L.: Advances in laser-based isotope ratio measurements: Selected applications, Appl. Phys. B-Lasers O., 92, 439–449, doi:10.1007/s00340-008-3128-x, 2008.

Knohl, A. and Baldocchi, D. D.: Effects of diffuse radiation on canopy gas exchange processes in a forest ecosystem, J. Geophys. Res., 113, G02 023, doi:10.1029/2007JG000663, 2008.

Knohl, A. and Buchmann, N.: Partitioning the net CO_2 flux of a deciduous forest into respiration and assimilation using stable carbon isotopes, Global Biogeochem. Cy., 19, GB4008, doi:10.1029/2004GB002301, 2005.

Knohl, A., Werner, R. A., Geilmann, H., and Brand, W. A.: Kel-F^{TM} discs improve storage time of canopy air samples in 10-mL vials for CO_2-$\delta^{13}C$ analysis, Rapid Commun. Mass Sp., 18, 1663–1665, doi:10.1002/rcm.1528, 2004.

Knohl, A., Werner, R. A., Brand, W. A. ., and Buchmann, N.: Short-term variations in ^{13}C of ecosystem respiration reveals link between assimilation and respiration in a deciduous forest, Oecologia, 142, 70–82, doi:10.1007/s00442-004-1702-4, 2005.

Knohl, A., Søe, A. R. B., Kutsch, W. L., Göckede, M., and Buchmann, N.: Representative estimates of soil and ecosystem respiration in an old beech forest, Plant Soil, 302, 189–202, doi:10.1007/s11104-007-9467-2, 2008.

Kuzyakov, Y. and Gavrichkova, O.: Review: Time lag between photosynthesis and carbon dioxide efflux from soil: A review of mechanisms and controls, Glob. Change Biol., 16, 3386–3406, doi:10.1111/j.1365-2486.2010.02179.x, 2010.

Miller, J. B., Yakir, D., White, J. W. C., and Tansl, P. P.: Measurement of $^{18}O/^{16}O$ in the soil-atmosphere CO_2 flux, Global Biogeochem. Cy., 13, 761–774, doi:10.1029/1999GB900028, 1999.

Mohn, J., Werner, R. A., Buchmann, B., and Emmenegger, L.: High-precision $\delta^{13}CO_2$ analysis by FTIR spectroscopy using a novel calibration strategy, J. Mol. Struct., 834-836, 95–101, doi:10.1016/j.molstruc.2006.09.024, 2007.

Mohn, J., Zeeman, M. J., Werner, R. A., Eugster, W., and Emmenegger, L.: Continuous field measurements of delta ^{13}C-CO_2 and trace gases by FTIR spectroscopy., Isot. Environ. Healt. S., 44, 241–51, doi:10.1080/10256010802309731, 2008.

Moyano, F. E., Kutsch, W. L., and Rebmann, C.: Soil respiration fluxes in relation to photosynthetic activity in broad-leaf and needle-leaf forest stands, Agr. Forest Meteorol., 148, 135–143, doi:10.1016/j.agrformet.2007.09.006, 2008.

Mund, M.: Carbon pools of European beech forests (Fagus sylvatica) under different silvicultural management, Berichte des Forschungszentrums Waldökosysteme Reihe A, Band 189, 1–256, 2004.

Ogée, J., Peylin, P., Ciais, P., Bariac, T., Brunet, Y., Berbigier, P., Roche, C., Richard, P., Bardoux, G., and Bonnefond, J.-M.: Partitioning net ecosystem carbon exchange into net assimilation and respiration using $^{13}CO_2$ measurements: A cost-effective sampling strategy, Global Biogeochem. Cy., 17, 3901–3916, doi:10.1029/2002GB001995, 2003.

Oikawa, P., Sturtevant, C., Knox, S. H., Verfaillie, J., Huang, Y.-W., and Baldocchi, D. D.: Revisiting the Partitioning of Net Ecosystem Exchange of CO_2 into Photosynthesis and Respiration with Simultaneous Flux Measurements of $^{13}CO_2$ and CO_2, Soil Respiration and a Biophysical Model, CANVEG, Agr. Forest Meteorol., 234-235, 149–163, doi:10.1016/j.agrformet.2016.12.016, 2017.

Orlowski, N., Kraft, P., Pferdmenges, J., and Breuer, L.: Exploring water cycle dynamics by sampling multiple stable water isotope pools in a developed landscape in Germany, Hydrol. Earth Syst. Sc., 20, 3873–3894, doi:10.5194/hess-20-3873-2016, 2016.

Pataki, D. E., Ehleringer, J. R., Flanagan, L. B., Yakir, D., Bowling, D. R., Still, C., Buchmann, N., Kaplan, J. O., and Berry, J. A.: The application and interpretation of Keeling plots in terrestrial carbon cycle research, doi:10.1029/2001GB001850, 2003.

Paya, A. M., Grams, T. E. E., and Bauerle, T. L.: Seasonal dynamics of δ^{13}C of C-rich fractions from Picea abies (Norway spruce) and Fagus sylvatica (European beech) fine roots, Plant, Cell Environ., 39, 2004–2013, doi:10.1111/pce.12765, 2016.

Savage, K., Davidson, E. A., and Tang, J.: Diel patterns of autotrophic and heterotrophic respiration among phenological stages, Glob. Change Biol., 19, 1151–1159, doi:10.1111/gcb.12108, 2013.

Schnyder, H., Schäufele, R., and Wenzel, R.: Mobile, outdoor continuous-flow isotope-ratio mass spectrometer system for automated high-frequency ^{13}C- and ^{18}O-CO_2 analysis for Keeling plot applications, Rapid Commun. Mass Sp., 18, 3068–3074, doi:10.1002/rcm.1731, 2004.

Shim, J. H., Powers, H. H., Meyer, C. W., Knohl, A., Dawson, T. E., Riley, W. J., Pockman, W. T., and McDowell, N.: Hydrologic control of the oxygen isotope ratio of ecosystem respiration in a semi-arid woodland, Biogeosciences, 10, 4937–4956, doi:10.5194/bg-10-4937-2013, 2013.

Sturm, P., Eugster, W., and Knohl, A.: Eddy covariance measurements of CO_2 isotopologues with a quantum cascade laser absorption spectrometer, Agr. Forest Meteorol., 152, 73–82, doi:10.1016/j.agrformet.2011.09.007, 2012.

Sturm, P., Tuzson, B., Henne, S., and Emmenegger, L.: Tracking isotopic signatures of CO_2 at the high altitude site Jungfraujoch with laser spectroscopy: Analytical improvements and representative results, Atmos. Meas. Tech., 6, 1659–1671, doi:10.5194/amt-6-1659-2013, 2013.

Thermo Fisher Scientific: Delta Ray^{TM} Isotope ratio infrared spectrometer: Operating manual, Thermo Scientific, Bremen, 2014.

Thomson, J. J.: Rays of positive electricity, Nature, 79, 52–56, doi:10.1038/079052a0, 1908.

Tuzson, B., Mohn, J., Zeeman, M. J., Werner, R. A., Eugster, W., Zahniser, M. S., Nelson, D. D., McManus, J. B., and Emmenegger, L.: High precision and continuous field measurements of δ^{13}C and δ^{18}O in carbon dioxide with a cryogen-free QCLAS, Appl. Phys. B-Lasers O., 92, 451–458, doi:10.1007/s00340-008-3085-4, 2008.

Vardag, S. N., Hammer, S., Sabasch, M., Griffith, D. W. T., and Levin, I.: First continuous measurements of $\delta^{18}O$-CO_2 in air with a Fourier transform infrared spectrometer, Atmos. Meas. Tech., 8, 579–592, doi:10.5194/amt-8-579-2015, 2015.

Vogel, F. R., Huang, L., Ernst, D., Giroux, L., Racki, S., and Worthy, D. E. J.: Evaluation of a cavity ring-down spectrometer for in situ observations of $^{13}CO_2$, Atmos. Meas. Tech., 6, 301–308, doi:10.5194/amt-6-301-2013, 2013.

Wehr, R., Munger, J., Nelson, D., McManus, J., Zahniser, M., Wofsy, S., and Saleska, S.: Long-term eddy covariance measurements of the isotopic composition of the ecosystem–atmosphere exchange of CO_2 in a temperate forest, Agr. Forest Meteorol., 181, 69–84, doi:10.1016/j.agrformet.2013.07.002, 2013.

Wehr, R., Munger, J. W., McManus, J. B., Nelson, D. D., Zahniser, M. S., Davidson, E. A., Wofsy, S. C., and Saleska, S. R.: Seasonality of temperate forest photosynthesis and daytime respiration, Nature, 534, 680–683, doi:10.1038/nature17966, 2016.

Wendeberg, M., Richter, J. M., Rothe, M., and Brand, W. A.: Jena Reference Air Set (JRAS): A multi-point scale anchor for isotope measurements of CO_2 in air, Atmos. Meas. Tech., 6, 817–822, doi:10.5194/amt-6-817-2013, 2013.

Wenninger, J., Koeninger, P., and Schneider, P.: Isotopic characterization of snow variability in two mountainous catchments, black forest mountains, Germany, in: International symposium on water resource and environmental protection (ISWREP), pp. 1004–1007, 2011.

Werle, P. W.: Diode-laser sensors for in-situ gas analysis, in: Laser in environmental and life sciences: Modern analytical methods, edited by Hering, P., Lay, J. P., and Stry, S., pp. 223–243, Springer, Berlin, Heidelberg, doi:10.1007/978-3-662-08255-3_11, 2004.

Werner, C., Schnyder, H., Cuntz, M., Keitel, C., Zeeman, M. J., Dawson, T. E., Badeck, F. W., Brugnoli, E., Ghashghaie, J., Grams, T. E. E., Kayler, Z. E., Lakatos, M., Lee, X., Máguas, C., Ogée, J., Rascher, K. G., Siegwolf, R. T. W., Unger, S., Welker, J. M., Wingate, L., and Gessler, A.: Progress and challenges in using stable isotopes to trace plant carbon and water relations across scales, Biogeosciences, 9, 3083–3111, doi:10.5194/bg-9-3083-2012, 2012.

Wingate, L., Ogée, J., Cuntz, M., Genty, B., Reiter, I., Seibt, U., Yakir, D., Maseyk, K., Pendall, E. G., Barbour, M. M., Mortazavi, B., Burlett, R., Peylin, P., Miller, J., Mencuccini, M., Shim, J. H., Hunt, J., and Grace, J.: The impact of soil microorganisms on the global budget of $\delta^{18}O$ in atmospheric CO_2, Proceedings of the National Academy of Sciences, 106, 22 411–22 415, doi:10.1073/pnas.0905210106, 2009.

Yakir, D. and Sternberg, L. d. S. L.: The use of stable isotopes to study ecosystem gas exchange, Oecologia, 123, 297–311, doi:10.1007/s004420051016, 2000.

Yakir, D. and Wang, X.-F.: Fluxes of CO_2 and water between terrestrial vegetation and the atmosphere estimated from isotope measurements, Nature, 380, 515–517, 1996.

Zhang, J., Griffis, T. J., and Baker, J. M.: Using continuous stable isotope measurements to partition net ecosystem CO_2 exchange, Plant, Cell Environ., 29, 483–496, doi:10.1111/j.1365-3040.2005.01425.x, 2006.

Zobitz, J., Keener, J., Schnyder, H., and Bowling, D. R.: Sensitivity analysis and quantification of uncertainty for isotopic mixing relationships in carbon cycle research, Agr. Forest Meteorol., 136, 56–75, doi:10.1016/j.agrformet.2006.01.003, 2006.

~~Frequency distributions of 300 measurements (each 1 s long) of a gas tank with pressurized air with known concentration and δ values ('PA-tank', c.f. Table 3).The black lines mark the respective means of all measurements and the area shaded in dark gray shows the expected uncertainty range based on the uncertainties of calibration tanks (only 0.01 for $\delta^{13}C$, thus not visible on this scale). The blue lines show the values that were measured with an independently calibrated instrument at the field site with their corresponding uncertainties in light gray.~~

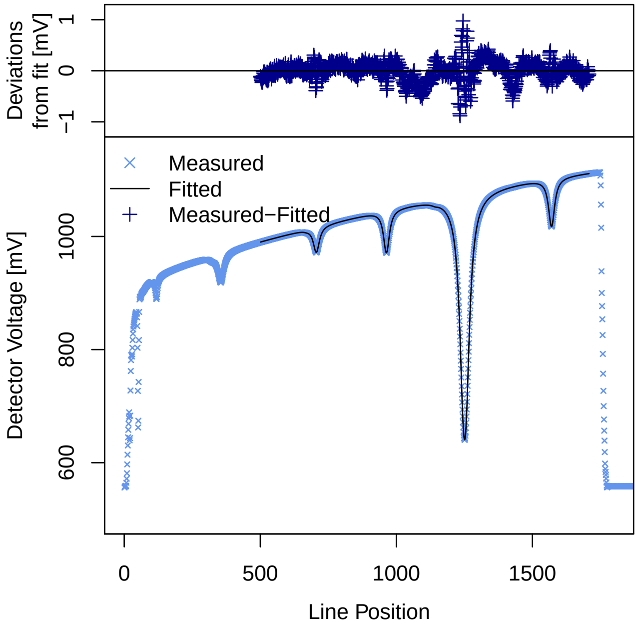

Figure 1. Measured and fitted spectrum, as exported from the instrument's operational software QTEGRA.

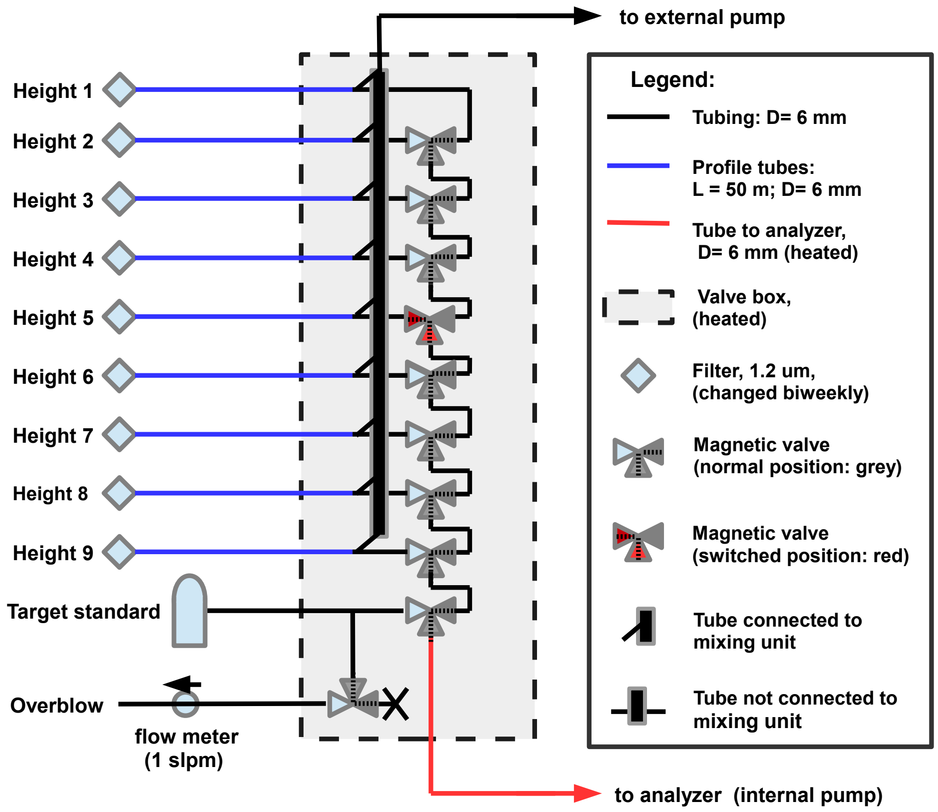

Figure 2. Plumbing scheme for the measurements of nine heights and a target standards, the example shows the valve positions when height 5 is sampled.

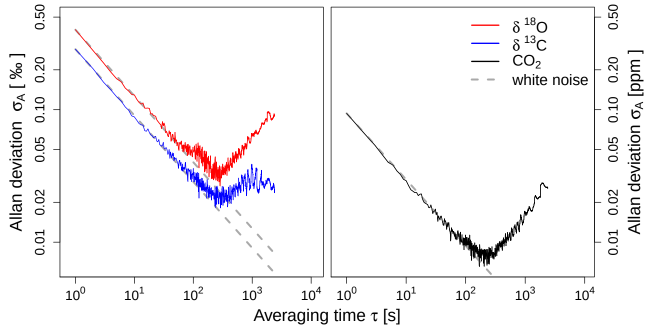

Figure 3. Allan deviation σ_A in ‰ VPDB for ^{13}C; in ‰ ~~VPDB-CO2~~ VPDB-CO$_2$ for ^{18}O and in ppm for CO$_2$ concentration, solid lines show the calculated Allan deviation and ~~the~~ dashed ~~line shows~~ lines show the typical white frequency noise error scaling.

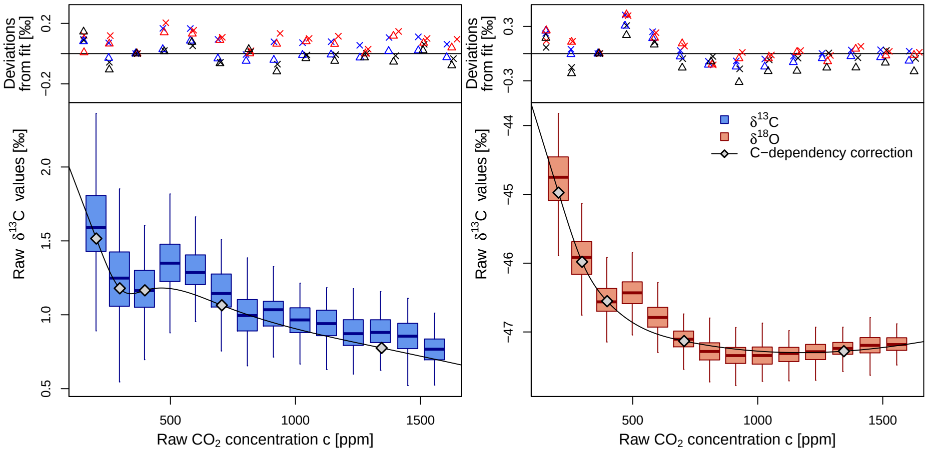

Figure 4. Box whiskers plots showing the nonlinear concentration-dependency (c-dependency) of raw δ values for ^{13}C and ^{18}O respectively, here as an example for the CO$_2$ tank 'ambient'. The measured c-dependency is compared to the respective c-dependency correction (black line, with grey symbols marking the data points used during the corresponding calibration measurement). The c-dependency correction is Offset-corrected to match the raw δ values at 400 ppm and the mean deviation from the offset-corrected fit is shown in the top panel for two measurements (different symbols) with three different gas tanks ('ambient' in blue, 'bio' in black and 'bio2' in red).

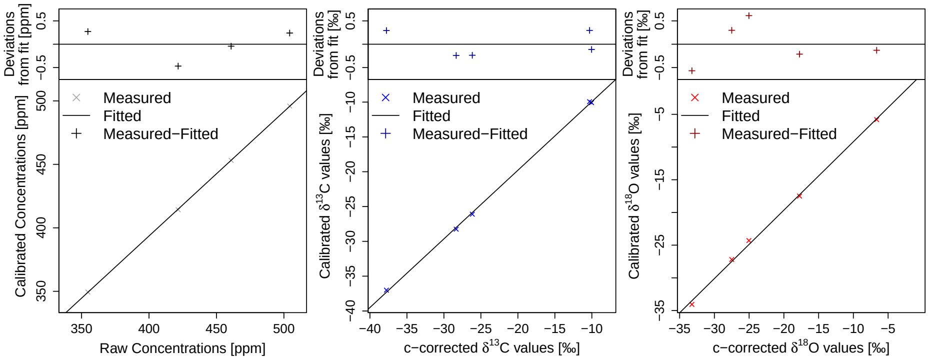

Figure 5. Linear calibrations for concentration (left panel) and concentration corrected δ^{13}C respectively δ^{18}O (middle and right panel).

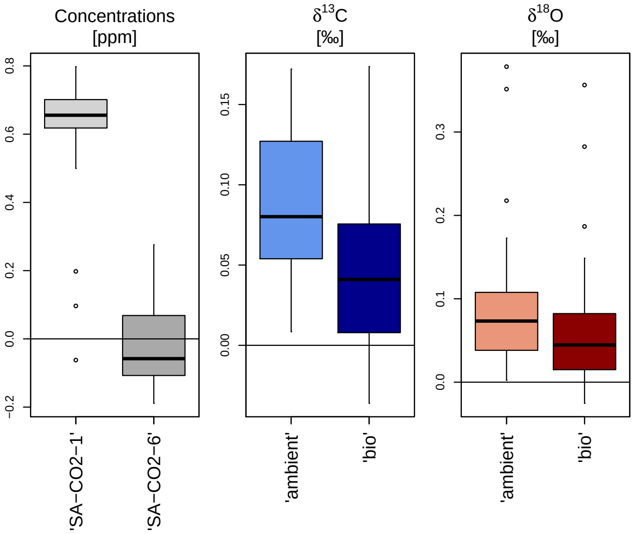

Figure 6. Box whiskers plots for the deviations of calibrated concentrations and δ values from laboratory measurements (at MPI in Jena) for repeated measurements of different calibration tanks (c.f. Table 3 for c and δ values of the gas tanks) over a period of 9 days (N=36). Delta values were measured at 400 ppm and 'referencing' was done approximately very 30 minutes at 380 ppm to simulate conditions during a measurement campaign.

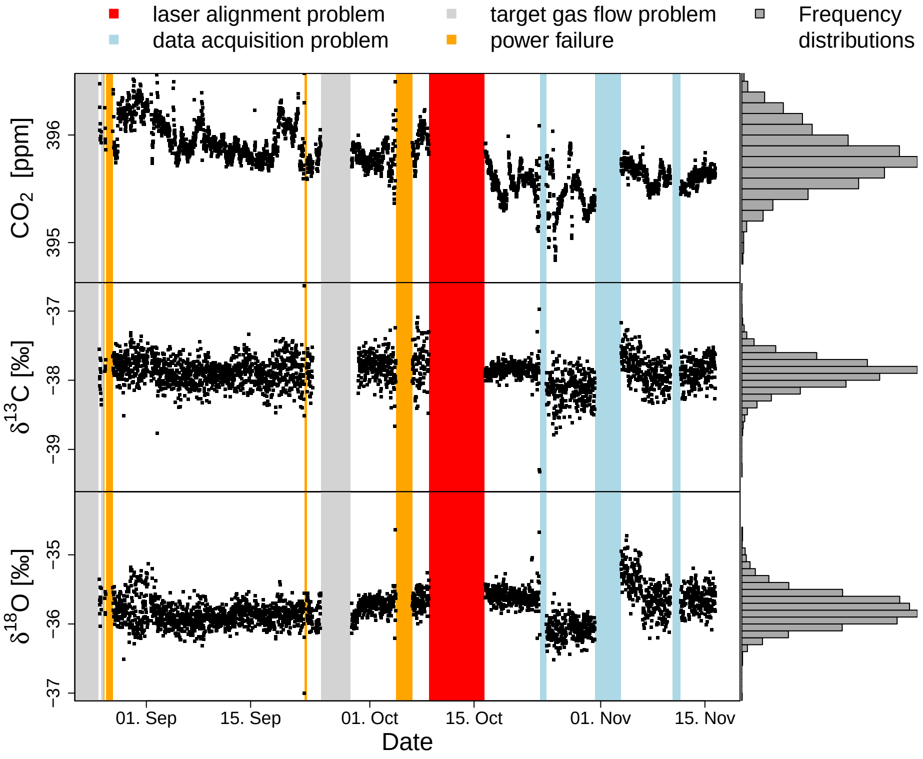

Figure 7. Time series and frequency distributions of half-hourly ~~performed~~ measurements of the concentration (top panel) and δ values (middle and bottom panel) for target gas '~~SA-CO2-5~~SA-CO$_2$-5' (c.f. Table 3) for the whole measurement period excluding periods that show problems with target gas flow, calibration and a laser alignment problem. Major reasons for data gaps are marked with different colors.

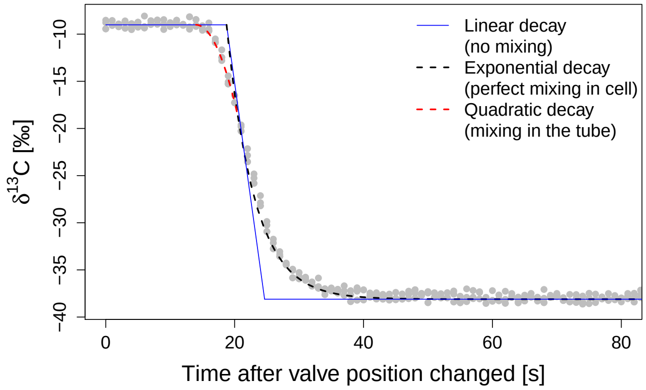

Figure 8. The ~~turnover behavior~~ response time of our experimental setup can be divided into three phases with different dominant ~~turnover~~ mechanisms: Directly after switching it took approximately 14 s to flush the tubing, the adjacent 4 s were dominated by the mixing processes in the tubes before the gas entered the measuring cell (quadratic fit) and finally we observed a ~~turnover~~ response behavior that is dominated by mixing processes within the measuring cell (exponential fit) with a characteristic decay time of $\tau_{10\%} = 10$ s for δ^{13}C. ~~The turnover was~~ These response times were similar for δ^{18}O (not shown). The linear fit shown here describes a first order approximation of the theoretical cell response for the (unrealistic) assumption that there is no mixing in the measurement cell. From this assumption, it can be derived that the δ values would show a dominantly linear decay with the slope $m = (\delta_{\mathrm{new}} - \delta_{\mathrm{old}})/\tau_{\mathrm{theoretical}}$ with the theoretical instrument cell response time $\tau_{\mathrm{theoretical}} = p * V/\Phi$, with pressure p, Volume V and flow rate Φ. In our case $\delta_{\mathrm{new}} - \delta_{\mathrm{old}}$= -29 ‰ and thus $\tau_{\mathrm{theoretical}}$= 5.9 s.

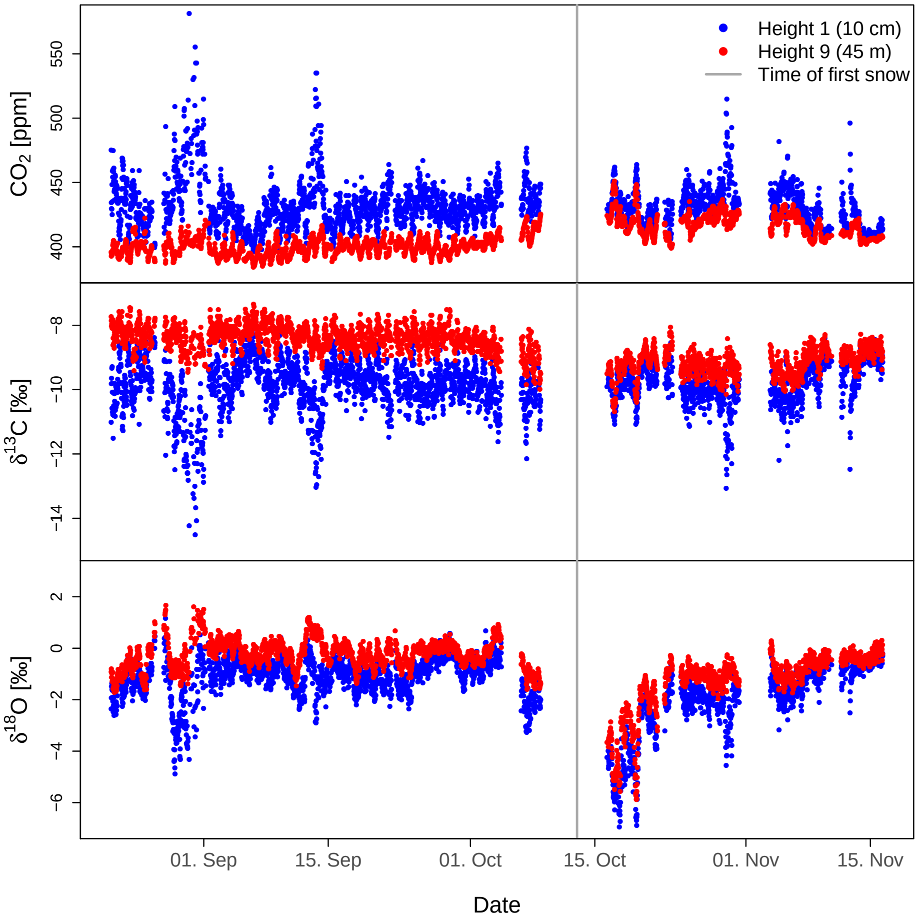

Figure 9. Time series of all measured concentrations c and both δ values at the lowest (blue points) and highest (red points) inlet in 0.1 and respectively 45 m height.

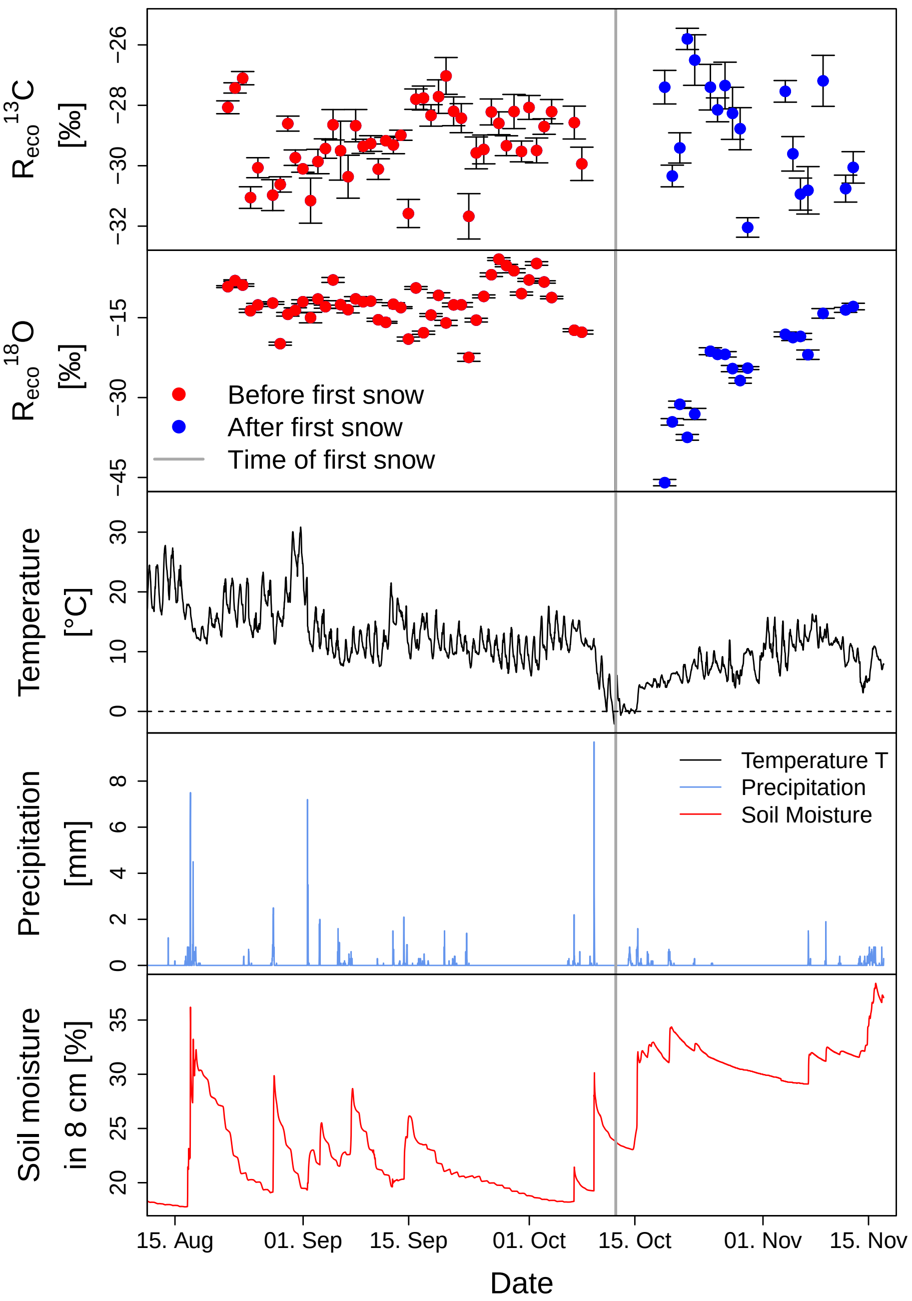

Figure 10. Time series of the measured isotopic composition of nighttime ~~Keeling-Plot intercepts δ^{13}~~CO$_2$ exchange (respiration) R^{13}_{eco}C ~~KP~~ and ~~δ^{18}~~ R^{18}_{eco}O ~~KP~~ based on Keeling-Plot intercepts in combination with temperature, precipitation and soil moisture in 8 cm depth. Error bars denote the standard error of the Keeling-Plot intercept (based on the linear regression of δ vs. $1/c$). A particular feature of this time series is a first snow and frost event on 13. October 2015, marked in gray.

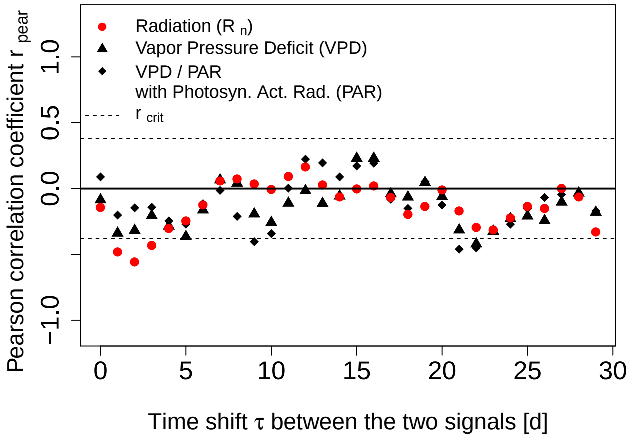

Figure 11. ~~The~~ Pearson correlation coefficient of ~~nighttime δ^{13}~~ the isotopic composition of ecosystem respiration R^{13}_{eco}C ~~$_{\mathrm{KP}}$~~ and the two-day-sum of different meteorological variables (shifted by different times τ) before the first snow event in autumn 2015.~~Error bars denote the standard error of the Keeling-Plot intercept (based on the linear regression of δ vs. $1/c$).~~

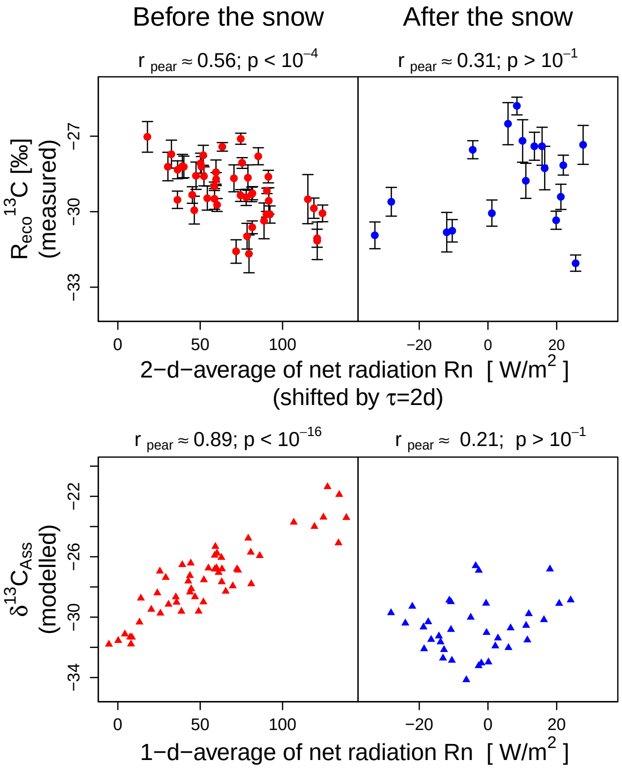

Figure 12. Observed relationships between net radiation R_n and the measured ~~nighttime Keeling-Plot intercepts δ^{13}~~isotopic composition of ecosystem respiration R^{13}_{eco}C ~~KP~~(top panels) and the modeled ^{13}C composition of assimilated material $\delta^{13}\mathrm{C}_{\mathrm{Ass}}$ (bottom panels). Significant correlations were observed before the first snow (left) but became insignificant after the snow (right). r_{pear} and p values are derived from the respective linear regressions.

Table 1. Nomenclature and abbreviations used in this publication, numbers for reference standards R_{std} from International Atomic Energy Agency (1995)

Stable isotope specific nomenclature	
R_{std}	Isotope ratio $C_{\mathrm{heavy}}/C_{\mathrm{light}}$ of an (arbitrary) reference standard
δ value	Relative deviation of the measured isotope ratio from R_{std}
VPDB	Vienna Pee Dee Belemnite - standard for ^{13}C ($R_{\mathrm{VPDB}}\approx 0.01124$)
VPDB-CO_2	Vienna Pee Dee Belemnite - standard for ^{18}O ($R_{\mathrm{VPDB-CO2}}\approx 0.0020883$)
Nomenclature	
σ_A	Allan deviation
R_n	Net radiation
RH	Relative humidity
VPD	Vapor pressure deficit
δ_{KP}	Keeling-Plot intercept
R_{eco}	Isotopic composition of nighttime CO_2 exchange (respiration) integrated over the ecosystem
Technical abbreviations	
IRIS	Isotope Ratio Infrared Spectrometer
IRMS	Isotope Ratio Mass Spectrometer
OA-ICOS	Off-axis Integrated Cavity Output Spectroscopy
CRDS	Cavity Ring Down Spectroscopy

Table 2. Examples for different optical instruments that measure the isotopic composition of CO_2 and reported values for minimal Allan deviations σ_A and the corresponding averaging times $\tau_{\min}$ (if available), see also Table 2 of the review of Griffis (2013).

Broadband light source based instruments	
Instrument:	Fourier Transform Infrared Spectrometer: Spectronus analyzer, *Ecotech Pty Ltd., Australia*
Minimal Allan deviation for δ^{13}C :	$\sigma_A(\tau_{\min}\approx 6000\ \mathrm{s})=0.01$ ‰ (Griffith et al., 2012)
Minimal Allan deviation for δ^{18}O :	$\sigma_A(\tau_{\min}\approx 7200\ \mathrm{s})=0.1$ ‰ (Vardag et al., 2015)
Instrument:	Fourier Transform Infrared Spectrometer: Nicolet Avatar, *Thermo Electron, USA*
Minimal Allan deviation for δ^{13}C :	$\sigma_A(\tau_{\min}\approx 960\ \mathrm{s})=0.15$ ‰ (Mohn et al., 2007)
Laser based direct absorption spectrometers in mid infrared	
Instrument:	Quantum cascade laser absorption spectrometer: QCLAS *Aerodyne Research Inc., USA*
Minimal Allan deviation for δ^{13}C :	$\sigma_A(\tau_{\min}\approx 100\ \mathrm{s})=0.01$ ‰ (Wehr et al., 2013); $\sigma_A(\tau_{\min}\approx 100\ \mathrm{s})=0.06$ ‰ (Sturm et al., 2012)
Minimal Allan deviation for δ^{18}O :	$\sigma_A(\tau_{\min}\approx 100\ \mathrm{s})=0.06$ ‰ (Sturm et al., 2012)
Instrument:	Lead-salt tunable diode laser absorption spectrometer: TGA100A/200, *Campbell Scientific Inc., USA*
Minimal Allan deviation:	no data for uncalibrated minimal σ_A, ideal averaging time $\tau_{\min}\approx 30$ s (Bowling et al., 2003c)
High frequency Allan deviation:	$\sigma_A(\tau=0.1\ \mathrm{s})=1.5$ ‰ for δ^{13}C and 2.2 ‰ for δ^{18}O (Bowling et al., 2003c)
Instrument:	Isotope Ratio Infrared Spectrometer: Delta Ray, *Thermo Scientific Inc., USA*
Minimal Allan deviation for δ^{13}C :	$\sigma_A(\tau_{\min}\approx 500\mathrm{s})=0.04$ ‰ (Geldern et al., 2014); $\sigma_A(\tau_{\min}\approx 300\,s)=0.02$ ‰ (this study, table 5)
Minimal Allan deviation for δ^{18}O :	$\sigma_A(\tau_{\min}\approx 300\mathrm{s})=0.04$ ‰ (this study, table 5)
Laser based path length enhanced absorption spectrometers in near infrared	
Instrument:	Cavity Ringdown Spectrometer: G1101-i+, *Picarro Inc., USA*
Minimal Allan deviation for δ^{13}C :	$\sigma_A(\tau_{\min}\approx 3600\ \mathrm{s}) \leq 0.1$ ‰ (Vogel et al., 2013)
Instrument:	Off-Axis Integrated Cavity Output Spectrometer: CCIA DLT-100, *Los Gatos Research Inc., USA*
Minimal Allan deviation for δ^{13}C :	$\sigma_A(\tau_{\min}\approx 200\ \mathrm{s})=0.04$ ‰ (at approximately 20 000 ppm CO_2) (Guillon et al., 2012); $\sigma_A(\tau_{\min}\approx 200\ \mathrm{s})=0.6$ ‰ (at approximately 2 000 ppm CO_2) (Guillon et al., 2012)
Laser based path length enhanced absorption spectrometers in mid infrared	
Instrument:	Quantum cascade laser absorption spectrometer: CCIA-48, *Los Gatos Research Inc., USA*
Minimal Allan deviation for δ^{13}C :	$\sigma_A(\tau_{\min}\approx 300\ \mathrm{s})=0.06$ ‰ (Oikawa et al., 2017)
Minimal Allan deviation for δ^{18}O :	$\sigma_A(\tau_{\min}\approx 300\ \mathrm{s})=0.04$ ‰ (Oikawa et al., 2017)

Table 3. Known CO_2-concentrations c and δ values for gas tanks used for calibration and instrument performance measurements. All measured concentrations and δ values refer to measurements that were done at Max-Planck Institute for Biogeochemistry in Jena and the δ^{13}C-values of the two pure CO_2 tanks. The pure CO_2 tanks 'bio' and 'ambient' were additionally measured with IRMS at Geoscience Center in Göttingen (Isotope Geology Division, Göttingen University) for their ^{13}C composition. Abbreviations for the purpose of the tanks: cCAL=concentration calibration; dCAL=δ-calibration; REF=referencing; EC=evaluating calibration ; pcCAL=post concentration calibration; REP=repeatability measurement

Gas tank	Used for	c [ppm]	δ^{13}C [‰VPDB]	δ^{18}O [‰VPDB-CO_2]
Pure CO_2 'ambient'	dCAL, REF, EC	-	-9.94 ± 0.01	-17.5 ± 0.3
Pure CO_2 'bio'	dCAL, EC	-	-28.25 ± 0.01	-27.2 ± 0.3
Pure CO_2 'bio-2'	EC	-	-26.1 ± 0.3	-24.3 ± 0.3
Pressurized air 'PA-tank'	pcCAL, EC	413.7 ± 0.2	-9.7 ± 0.2	-5.3 ± 0.4
Syn. air with CO_2 'SA-CO_2-1'	cCAL, pcCAL, EC	349.5 ± 0.1	-37.01 ± 0.02	-34.1 ± 0.4
Syn. air with CO_2 'SA-CO_2-2'	cCAL, pcCAL	453.9 ± 0.1	-36.98 ± 0.02	-34.2 ± 0.6
Syn. air with CO_2 'SA-CO_2-3'	pcCAL	349.6 ± 0.1	-37.02 ± 0.01	-34.3 ± 0.4
Syn. air with CO_2 'SA-CO_2-4'	pcCAL, EC	453.2 ± 0.1	-37.02 ± 0.02	-34.8 ± 0.4
Syn. air with CO_2 'SA-CO_2-5'	pcCAL, REP	396.5 ± 0.1	-37.02 ± 0.02	-34.7 ± 0.2
Syn. air with CO_2 'SA-CO_2-6'	EC	496.0 ± 0.1	-37.02 ± 0.02	-34.8 ± 0.1

Table 4. Validation of the multilayer model CANVEG using Eddy Covariance measurements of gross primary productivity GPP, net ecosystem exchange NEE, latent and sensible heat flux LE and H. Slopes, R^2 values and normalized standard error estimates NSEE of linear regressions between modeled and measured values are comparable to the numbers given by (Knohl and Baldocchi, 2008).

	SLOPE	R^2	NSEE
GPP	0.92	0.90	0.26
NEE	0.97	0.92	0.28
LE	1.03	0.78	0.16
H	0.96	0.87	0.37

Table 5. Allan deviation σ_A for different averaging times τ, with the minimum Allan deviation for $\tau_{\min} \approx 290\,s$ for both δ-values and 170 s for CO_2 concentration c

τ [s]	$\delta^{13}C$ [‰]	$\delta^{18}O$ [‰]	c [ppm]
1	0.29	0.40	0.09
20	0.06	0.09	0.02
80	0.03	0.05	0.02
$\tau_{\min}$	0.02	0.03	0.007
500	0.03	0.04	0.01
1800	0.03	0.08	0.01

Table 6. Uncertainties related to the different calibration steps and their repeatability defined as 1σ standard deviation of the respective calibration step.

Calibration	$\delta^{13}C$ [‰]	$\delta^{18}O$ [‰]	c [ppm]
Linear calibrations	0.24	0.3	0.45
corresponding repeatability	0.05	0.1	0.2
Correction of c-dependency	0.2	0.4	-
corresponding repeatability	0.15	0.15	-

Table 7. Standard deviations σ of the measured (calibrated) δ values over a large concentration range based on 6 hourly lab measurements over a period of nine days.

Concentration ppm	$\sigma(\delta_{\mathrm{meas}} - \delta_{\mathrm{tank}})$ ‰			
	tank: 'ambient'		tank: 'bio'	
	^{13}C	^{18}O	^{13}C	^{18}O
202	0.07	0.14	0.09	0.13
396	0.04	0.05	0.08	0.08
600	0.09	0.08	0.12	0.12
807	0.08	0.08	0.11	0.11
1018	0.10	0.08	0.13	0.11
1232	0.12	0.09	0.13	0.11
1450	0.14	0.11	0.15	0.12
1664	0.14	0.11	0.14	0.12
3145	0.17	0.15	0.17	0.15

Table 8. Percentage of total measurement time for major data gaps. The latter two data gaps concerned only target gas measurements.

Reason for data gap	Percentage
Data acquisition problems	6.0 %
Laser alignment problem	8.6 %
Calibration	1.5 %
Power failures	3.3 %
Additional measurements	1.6 %
Plumbing issues (only target)	9.5 %
Switching unit failure (only target)	0.7 %

Table 9. R^2 values for correlations between the ^{18}O composition of nighttime CO_2 exchange R^{18}_{eco}O and different meteorological variables. Significance thresholds are given by *** for $p<10^{-4}$; ** for $p<10^{-3}$ and * for $p<10^{-2}$. For some parameters the height above the ground (with negative values indicating the depth below the ground) is given in brackets, the parameters without such indication are measured 42 m above the ground.

	All periods	Before the snow	After the snow
Soil moisture (-8 cm)	0.49 ***	0.04	0.00
Upwards shortwave radiation	0.40 ***	0.28 *	0.04
VPD	0.18 **	0.09	0.22
Soil temperature (-8 to -64 cm)	0.36 ***	0.06	0.70 ***
Air Temperature	0.22 **	0.02	0.61 **
Air Temperature (2 m)	0.21 **	0.05	0.60 **
Upwards longwave radiation	0.20 **	0.02	0.61 **
Incoming longwave radiation	0.05	0.49 ***	0.03
Ambient pressure	0.05	0.39 ***	0.36 *
Incoming shortwave radiation	0.39 ***	0.23 **	0.13
Dewpoint temperature	0.02	0.38 ***	0.14
Specific humidity	0.02	0.34 ***	0.17
H_2O concentration	0.02	0.34 ***	0.17
Actual vapor pressure	0.02	0.33 ***	0.18
Relative humidity	0.28 ***	0.31 ***	0.15
Rain	0.01	0.28 **	0.05

Appendix A: Measures to improve data quality

To reduce the uncertainty of the calculated isotopic composition of ~~ecosystem respiration~~nighttime CO_2 exchange (respiration) R^{13}_{eco}C and R^{18}_{eco}O, we used the following approaches concerning setup and post-processing.

- **Minimizing the sampling time**

  One of the key assumptions of the Keeling-Plot approach Eq. (1) is the mixing of a constant background with one (integrated) source. This assumption is justified ~~,~~ if there is no significant change in the background concentration c_{bg}, its isotopic composition δ_{bg}, and the isotopic composition of the (integrated) source δ_s for all data points that are taken into account for a single Keeling-Plot. For the case of an integrated source, a constant δ_s can be ensured when the isotopic composition of the individual source components ~~$\delta s, i$~~ $\delta_{s,i}$ as well as the relative contribution of the individual source components α_i in Eq. (2) are constant. As in general all these quantities ($\delta_{s,i}$, α_i, c_{bg} and δ_{bg}) can vary with time, this assumption tends to be violated stronger for longer measurement times. Thus, the uncertainty of calculated ~~Keeling plot~~ Keeling-Plot intercepts can be reduced by minimizing the measurement time, as discussed e.g. by Bowling et al. (2003b), who recommend to use only measurements that took less than five hours for analyzing Keeling-Plot intercepts for $\delta^{18}O$. As our setup measures all the nine heights within 30 minutes, we were ~~also~~ able to calculate Keeling-Plots for ~~even~~ shorter periods. During data analysis we calculated Keeling-Plots on timescales between 30 min and 5 h.

- **Increasing the CO_2 concentration range**

  The linear regression that underlies the Keeling-Plot, can be improved significantly by increasing the CO_2 concentration (Zobitz et al., 2006). In our setup, we increase the CO_2 concentration range by using data from all nine inlet heights within one Keeling-Plot, but this, on the other hand, could violate the assumption of constant relative contributions of the individual source components α_i in Eq. (2) to the integrated source. To analyze if there ~~are any biases~~ is any bias (which may have several contributions) due to the inclusion of the different inlet positions, we evaluated the Keeling-Plots for the lower inlets (heights 1-4) and for all all inlets (heights 1-9) separately. The difference Δ between the these ~~differently calculated~~ Keeling-Plot intercepts based on different data sets showed a symmetric frequency distribution around 0 (Fig. S1 in the supplementary material)~~and by~~. By including all heights into the data analysis, we ~~could reduce~~ reduced the error of the intercept σ ~~significantly~~ from a mean value of ~~$\overline{\sigma_{low}} \approx 1.5‰$~~$\overline{\sigma_{low}} \approx 1.5‰$ to $\overline{\sigma_{all}} \approx 0.8‰$ for both isotopic species. These numbers refer to ~~a Keeling-Plot that includes~~ Keeling-Plots that include data from three consecutive measurement cycles, yielding a temporal resolution of 90 min. Reasons for the choice of this time resolution are given below.

- **Performing an ordinary Model I regression instead of a Model II regression**

  We used an ordinary Model I regression instead of a Model II regression. According to Zobitz et al. (2006), this approach takes into account that the error of the measured δ-values dominates over the error of the measured concentrations and yields unbiased estimates of the Keeling-Plot intercept. In our setup, the application of a Model I regression can be justified by the fact that the relative precision of δ measurements is more than an order of magnitude larger than the relative precision of the CO_2 concentration measurements: To estimate the relative ~~uncertainty~~ precision of the three measured quantities, we calculated the ratio of Allan Deviation at our measurement time of 20 s over the typical range of c, δ^{13}C and δ^{18}O. The typical range, we further define as the median of the ~~range we obtained in one of our~~ ranges that were obtained during the 30 ~~min~~ minutes measurement cycles. Thus, with ~~Allan deviations of 0.02 ppm, 0.06 and 0.09 and~~ the Allan deviations in Table 5 and with typical ranges of 26 ppm, 1.5‰ and 1.1 ‰ for c, δ^{13}C and δ^{18}O, ~~we get relative precisions in the order of 10^{-3} for~~ the relative precision for the obtained variability in CO_2~~10^{-2} for~~, δ^{13}C ~~to~~

~~10^{-1} for~~ and δ^{18}O is in the order of 10^{-3}, 10^{-2} and 10^{-1}, respectively. Thus, the relative precision of the concentration measurement is at least an order of magnitude better than the relative precision of ~~concentration~~ δ measurements.

- **Filtering data to get only high quality linear regressions**

  Data filtering to remove bad quality and biased (Model II) linear regressions has been often done by excluding data with a to low CO_2 concentration range (Pataki et al., 2003; Bowling et al., 2005). Whereas Pataki et al. (2003) recommend to exclude all data from the analysis that spans a CO_2 range below 75 ppm, Bowling et al. (2005) choose this threshold to be 40 ppm. This data filtering approach, based on CO_2 concentration range, does not seem necessary when applying a Model I regression: Zobitz et al. (2006) analyzed consequences of small CO_2 concentration ranges ~~numerical~~ numerically as well as ~~analytical~~ analytically and conclude that for Keeling-Plot intercepts based on Model I regressions 1) a bias at low CO_2 concentration ranges ~~in~~ is not expected at current analytical error levels and 2) that errors in the intercept can be small, even for small CO_2 concentration ranges if the δ-values are measured accurately enough. Figure S2 in the supplementary material shows the relationship between CO_2 concentration range and the standard error of the intercept σ for a measurement period of 30 minutes. This figure also shows two comparable approaches for data filtering that both accept 85 % of the data: One approach would be to directly remove data with large intercept errors, and the other approach, as mentioned above, is to remove data with to low CO_2-range. As visible in Fig. S2 in the supplementary material, this approach would remove considerable amounts of data with a very small standard error of the intercept σ, which might be good quality data. For this reason (and as we do not expect a bias occurring for small CO_2 concentration ranges for our Model I type regression), we decide for a direct filtering based on a σ-threshold and used the 85 % data points with the smallest standard error σ. The filtered nighttime Keeling-Plot intercepts based on 90 minutes of data acquisition had R^2 values with a median of 0.87 and 0.81 for ^{13}C and ^{18}O with mean values of 0.85 and 0.77 and standard deviations σ of 0.1 and 0.16 respectively. Example Keeling-Plots with R^2 values spanning the range of mean $\pm 1\sigma$ are provided in the supplementary material (Figure S5 in the supplementary material).

- **Removing outliers**

  Our set-up, based on the measurement of δ^{13}C, δ^{18}O and CO_2 concentration c, enabled us ~~in principal~~ to calculate individual Keeling-Plots based on all ~~inlets~~ inlet heights (heights 1-9) with a temporal resolution of 30 min. We calculated Keeling-Plots on different timescales ranging from 30 min to 5 h by using one to ten measurement cycles and evaluated how the ~~calculated~~ Keeling-Plot intercepts $\delta^{13}C_{KP}$ and the corresponding standard errors of the linear regression σ changed (Fig. S3 in the supplementary material). ~~As expected, the error of the intercept σ could be reduced by including more measurement cycles.~~ Additionally, the ~~range of calculated~~ calculation of Keeling-Plot intercepts ~~reduced considerably:~~ based on longer timescales increased the number of Keeling-Plot ~~intercepts that are based on 30 min timescales included much more data points far beyond the range of Keeling Plot Intercepts on longer timescales. For timescales of 2 h to 5 h there were only few data points with Keeling plot intercepts below~~ intercepts within reasonable ranges. For Keeling-Plots that were averaged over 2h (5h), a fraction of 97% (99%) of the Keeling Plot intercepts were between -33 ~~–and above~~ and -25 ~~, which would also be unreasonable numbers: For a timescale of 2 h 3 % of the total calculated data points were out of this range, whereas for timescales of 5 h only 1 %of~~ ‰. Because the ~~data points were outside of this range. As the~~ range of the Keeling-Plot intercepts should not depend on the chosen timescale, we considered the Keeling-Plot intercepts that were outside of this range as outliers and removed them from ~~the consecutive data analysis~~ further analysis (also for Keeling-Plot Intercepts that were based on shorter timescales).

- **Choosing a time resolution for individual Keeling-Plots**

  To decide for a suitable time resolution to analyze the temporal variability of the Keeling-Plot intercepts, we had to solve the ~~threshold~~ trade-off between 1) more accurate data on longer timescales and 2) a larger number of data points that were available (after the above mentioned filtering procedures). We decided to fit the individual Keeling Plots on 90 min resolution, which ~~yield~~ yields a maximal number of N~~$_{\text{filtered}} \approx 2350$~~ $_{\text{filtered}} \approx 2300$ accepted data points and ~~standard errors σ with~~ a median of 0.76 ‰ for the standard errors σ (Fig. S4 in the supplementary material).

- **Calculation of weighted means for nighttime data**

  For analyzing variations in the ~~ecosystems respiration~~nighttime CO_2 exchange (respiration) R_{eco} on seasonal timescales we used the (filtered) individual Keeling-Plots, each based on 90 minutes of input data, and calculated the mean over all Keeling-Plots that were collected between ~~9h30 pm~~ 21h30 and 2h30 ~~am~~ (using the weight w based on with the standard error σ of the Keeling-Plot intercept: $w = 1/\sigma^2$).